

SAND81-1180  
Unlimited Release  
UC-62

# A User's Guide to Helios: A Computer Program for Modeling the Optical Behavior of Reflecting Solar Concentrators

## Part I. Introduction and Code Input

Charles N. Vittitoe, Frank Biggs

Prepared by Sandia National Laboratories, Albuquerque, New Mexico 87185  
and Livermore, California 94550 for the United States Department of Energy  
under Contract DE-AC04-76DP00789.

Printed August 1981

***When printing a copy of any digitized SAND  
Report, you are required to update the  
markings to current standards.***



Sandia National Laboratories

Issued by Sandia National Laboratories, operated for the United States Department of Energy by Sandia Corporation.

**NOTICE:** This report was prepared as an account of work sponsored by an agency of the United States Government. Neither the United States Government nor any agency thereof, nor any of their employees, nor any of their contractors, subcontractors, or their employees, makes any warranty, express or implied, or assumes any legal liability or responsibility for the accuracy, completeness, or usefulness of any information, apparatus, product, or process disclosed, or represents that its use would not infringe privately owned rights. Reference herein to any specific commercial product, process, or service by trade name, trademark, manufacturer, or otherwise, does not necessarily constitute or imply its endorsement, recommendation, or favoring by the United States Government, any agency thereof or any of their contractors or subcontractors. The views and opinions expressed herein do not necessarily state or reflect those of the United States Government, any agency thereof or any of their contractors or subcontractors.

Printed in the United States of America  
Available from  
National Technical Information Service  
U. S. Department of Commerce  
5285 Port Royal Road  
Springfield, VA 22161

NTIS price codes  
Printed copy: \$7.00  
Microfiche copy: A01

# **A User's Guide to Helios: A Computer Program for Modeling the Optical Behavior of Reflecting Solar Concentrators**

## **Part I. Introduction and Code Input**

Charles N. Vittitoe  
Frank Biggs  
Theoretical Division 4231  
Sandia National Laboratories  
Albuquerque, NM 87185

### **Abstract**

HELIOS is a flexible computer code for evaluating designs for central-receiver, parabolic-dish, and other reflecting solar-energy collector systems, for safety calculations on the threat to personnel and to the facility itself, for determination of how various input parameters alter the power collected, for design trade-offs, and for heliostat evaluations. Input variables include atmospheric transmission effects, reflector shape and surface errors, suntracking errors, focusing and alignment strategies, receiver design, placement positions of the tower and mirrors, and time of day and day of the year for the calculation. Complete input instructions and a description of the code structure are given in Part I. The Code is in use at Sandia National Laboratories, Albuquerque (SNLA) on CDC 6600, CYBER 76, and CDC 7600 computers.

## **Acknowledgment**

The authors thank P. Van Delinder and W. C. Burd for guidance in the DISSPLA plotting routines. C. S. Hoyle furnished the PLATE subroutine giving the facet shape that results from stress analysis. R. E. Jones provided the INTRP1, INTRYL, and VAL2D interpolation routines. S. L. Thompson contributed the CONTC2, CONSC2, and CLIPC2 routines used in contour plotting. J. R. Koteras supplied the gravity-loading data for Martin Marietta and McDonnell Douglas heliostat designs. Not only this document, but the HELIOS code itself benefited from our discussions with users of the code—especially F. Delgado, J. T. Holmes, D. L. King, D. J. Kuehl, L. K. Matthews and L. O. Seamons—and from results of their experiences with the code. R. E. Lighthill provided help through several programming dilemmas and aided in the addition of two-dimensional effective sunshapes to the code. The report was also improved by the critical reading of P. C. Kaestner.

## **Inquiries**

Requests for the HELIOS Code should be directed to the authors. DOE has given permission for unlimited distribution.

## **Caution**

The HELIOS Code is still under development. Although approaching its fifth birthday, the Code still suffers from some previous limitations. It is not optimized for speed. Many possible combinations of options have not yet been exercised. With the increased number of options, the speed is even more controlled by the actual choices made. Speed optimization should first be tried for those options most frequently used.

## Preface

This user's guide is an extensive revision of and replacement for the report SAND76-0346, *HELIOS: A Computer Program for Modeling the Solar Thermal Test Facility — A Users Guide*. The three editions of that report (March 1977, June 1977, and October 1978) were attempts to meet the need for user guides and to be reasonably current in documenting new code capabilities. A series of memoranda have documented improvements over the last 3 years. The guide describes these improvements and several additional capabilities now available in HELIOS and in its associated plotting and analysis codes. The HELIOS Code is on disk and magnetic tape at Sandia National Laboratories (SNL) Albuquerque, as FORTRAN source-card images in CDC UPDATE format.

The user's guide has been divided into a series of parts to reflect its anticipated use. Part I concentrates upon the input and is expected to receive the most use. Part II directs attention to the output for several sample problems. This portion will be useful mainly for learning details of the output that will become automatic after several actual uses of the Code. Part III gives a series of appendices concerning Code details such as subroutine and function descriptions and how the common blocks are used. This portion may be useful when the Code is altered to model more exotic collection systems. Other parts describe the plotting and data editing codes and how alterations may be made to treat special heliostat or receiver shapes not available as regular options in HELIOS. Most of the analytic basis for the HELIOS Code is described in SNL Report SAND76-0347. Parts of the user's guide include analytical descriptions of features not described in SAND76-0347 or elsewhere.

## Part I Contents

I	Introduction .....	9
II	Data Flow in HELIOS .....	11
III	HELIOS Input .....	19
	Group 1 Input Cards — Problem Type.....	19
	Group 2 Input Cards — Sun Parameters .....	21
	Concentrator Errors .....	25
	Sun-Tracking Errors.....	25
	Bounding Calculations .....	25
	Group 3 Input Cards — Receiver Parameters.....	26
	Group 4 Input Cards — Facet Parameters.....	31
	Group 5 Input Cards — Heliostat Parameters .....	33
	Group 6 Input Cards — Time Parameters .....	35
	Group 7 Input Cards — Atmospheric Parameters .....	36
IV	Interactive Preparation of Input File .....	37
V	CELL Code Preparation of Tape 3 for IHELD = 2.....	43
	Cell Geometry .....	43
	CELL Code Input and Output.....	46
	References.....	49
	APPENDIX A — Input Flow Charts .....	51
	APPENDIX B — CELL Code Listing.....	57

## Illustrations

### Figure

1	The CRTF at Sandia National Laboratories .....	10
2	Basic Flow for the Main Overlay, HELIOS 0,0 .....	12
3	Flow Diagram for Overlay 1, 0 — Program A .....	13
4	Flow Diagram for Overlay 5, 0 — Program D .....	14
5	Flow Diagram for Overlay 2, 0 — Program B .....	15
6	Flow Diagram for Overlay 3, 0 — Program C .....	16
7	Target Subdivision for NTARSH = 3 .....	30
8	Plane Projection of Facet Array on One Heliostat .....	32
9	Sample Heliostat Mounting .....	32
10	Heliostat Deployment in Tower Coordinate System .....	35
11	Data Organization for Tape 3 .....	44
12	Cell Boundary Geometry .....	45
13	Cell Angular Interval Geometry .....	45
14	Angular Limits for a Cell .....	45
15	Cell Structure Resulting From CELL Input as in Appendix B ...	47
16	Cell Structure With an Example of Heliostat Assignments .....	48

# A Users's Guide to Helios: A Computer Program for Modeling the Optical Behavior of Reflecting Solar Concentrators

## I. Introduction

A Central Receiver Test Facility (CRTF) is currently in operation at Sandia National Laboratories, Albuquerque, NM (SNLA). The many mirrors, shown in Figure 1, reflect power from the sun and concentrate it at the tower receiver.

A mathematical model has been developed to simulate the concentrators, and the computer code HELIOS was written to implement it. (The name HELIOS derives from that of the ancient Greek god of the sun.) The Code is flexible and has broad applications for proposed facility design evaluations, calibration checks, design trade-offs, and safety calculations showing exactly where the power is going and how various input parameters alter not only the power collected but also the threat to personnel and to the facility itself. To facilitate alterations and separate the numerous effects to be considered, the Code is structured with many subroutines. Comment cards are abundant for convenience of the user.

Various sections of the computer code use a series of coordinate systems:

- A sun-concentrator system, where the facet normal is  $z$  and the central incident ray is in the  $y, z$  plane
- The facet system, where the origin is at the facet center and coordinate directions are along the horizontal edge of the facet, along the orthogonal edge of the facet, and normal to the facet
- The heliostat system, which locates the centers of each facet relative to the center of the heliostat mounting

- The tower coordinate system, where the center of each heliostat mounting base is specified by the components (east, north, vertical) measured from the origin at the base of the tower receiver
- A target coordinate system, which is also used for convenient specification of the mesh of target points.

These coordinate systems are discussed in detail elsewhere.<sup>1</sup>

Effects included in the Code are declination of the sun; rotation of the earth; earth orbit eccentricity; molecular and aerosol scattering in several standard, clear atmospheres; atmospheric refraction; angular distribution of sunlight; reflectivity of the facet surface; shapes of focused facets; distribution of errors in the surface curvature and in aiming; facet orientation; and shadowing and blocking. Tower coordinates of heliostats can be input variables instead of variables restricted to those built into the Code.

Options are available for focusing the heliostats (i.e., aligning or canting the facets on the heliostats and adjusting their focal length, radius of curvature, or center pulldown distance for best power collection) independently at any day of the year and time of day, or for canting a heliostat on-axis.\* The facet shape may be chosen as flat, parabolic, or spherical; as

---

\*On-axis canting is done by artificially positioning the sun along the central ray to the prealignment (aim) point and adjusting each facet orientation so the central reflected ray passes through the prealignment point.

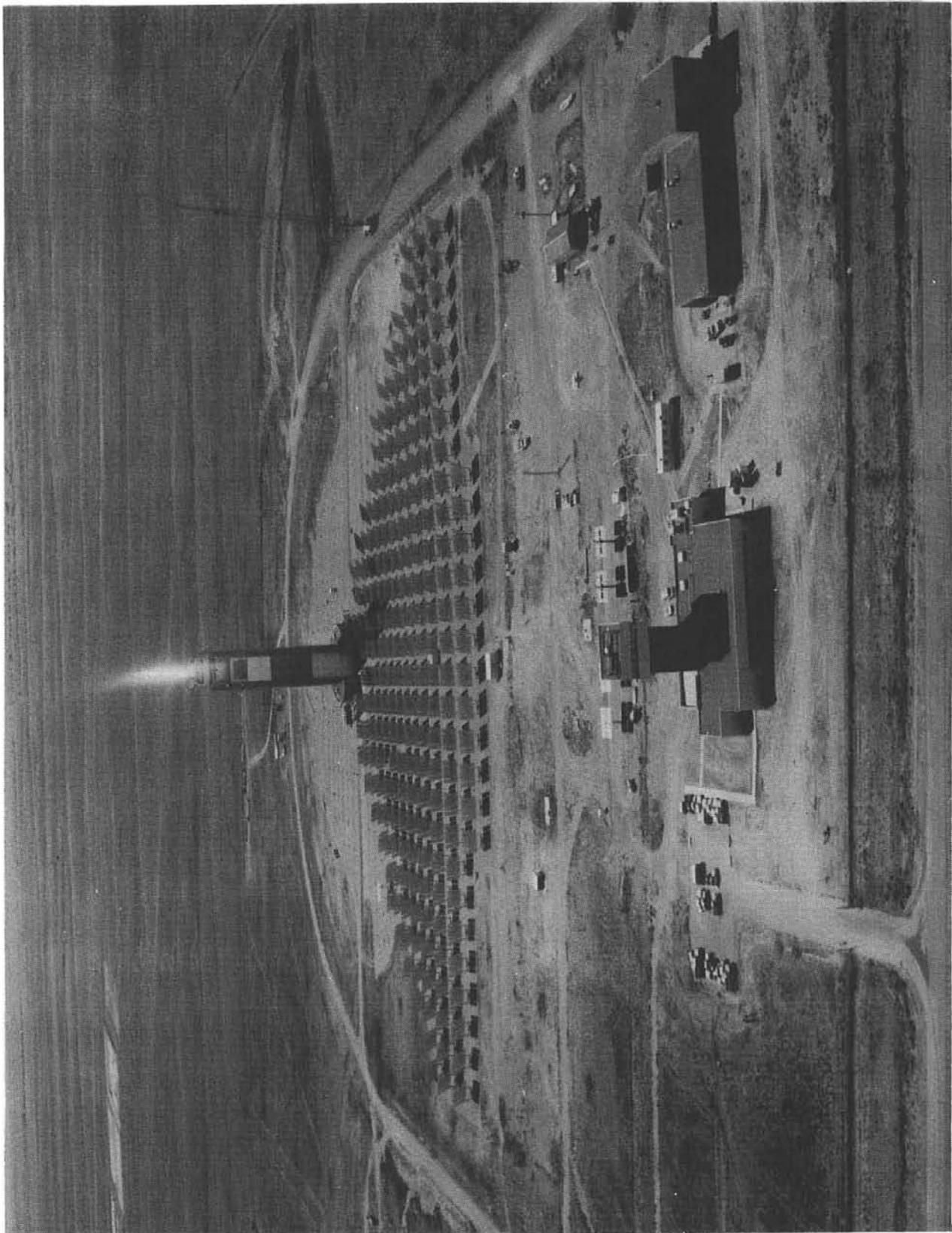


Figure 1. The CKTF at Sandia National Laboratories



that resulting from stress analysis;<sup>1</sup> or as a shape furnishing perfect focusing at all points on the facet surface and for all times. This perfect-focus option is convenient for efficient upper-limit calculations of collected power. The user can also furnish a subroutine to provide his own facet shape. Facet properties that might vary with temperature can be treated by a series of computer runs with differing input parameters.

A user may iterate on the same heliostat by using a series of focusing days or times of day to optimize the choice for that heliostat. The aim-point of the heliostat may be any spatial position; it is not confined to the point used for focusing the facets.

A mesh of target points may be chosen for three-dimensional (3-D) graphs of the flux density. Other choices give the power density from a facet, a heliostat, or a series of heliostats as a function of time of day. When the target surface is rectangular, spherical, or cylindrical, estimates are given for the power collected by the target and for its uncertainty. The flux-density incident upon the target may be separated into vector components for more detailed treatment of specific receivers. The angular distribution of incoming power may also be tabulated at each of 121 target points.

The series of effects not currently taken into account includes possible changes in aerosol scattering and absorption, wavelength and angle-of-incidence dependence of facet reflectivity, reflection from the front glass surface on each facet, the variation of the wavelength-dependent incident energy flux with the choice of atmosphere, and diffuse reflection from the facets (except by its effect on the distribution of errors). Each of these effects can be included by altering the appropriate subroutine. Some of the effects, such as variation with choice of atmosphere, are best treated by numerical fits to data from other work. A series of atmospheres could be chosen. Transmission calculations (with aerosols and absorption) for the sun's spectrum could then be used to generate a numerical fit of the incident energy flux as a function of the sun's zenith angle. An integration through the atmosphere would also generate refraction data. These data could then be inserted into the code with an option to specify which atmosphere is to be used. Some exotic effects that are now omitted include eclipse of the sun, bird, cloud, and airplane

shadowing, and atmospheric turbulence around the high-temperature receiver.

Data describing the sun shape and its insolation may be used as input variables appropriate to the local conditions. This information is available from measurements by the circumsolar telescope now in operation at the CRTF.<sup>2</sup> A series of other sunshape options are available.

A heliostat is "shadowed" when a shadow produced by other heliostats or by a tower falls upon it. The heliostat is "blocked" when its reflected rays are intercepted by another heliostat before reaching the target. At present, when a heliostat is shadowed or blocked by more than one object, either another heliostat or a tower receiver, the affected portions may be treated as overlapping either completely or not at all. Heliostats that are both shadowed and blocked are assumed to have overlapping of the affected portions. The overlapping assumption tends to overestimate the energy collected at certain target positions and is therefore useful for safety calculations. The nonoverlapping situation has been verified as appropriate for several times of the day between noon and 2 pm during the winter for targets near the usual CRTF receiver locations. Of course, for targets close to the ground, the nonoverlapping assumption would underestimate the collected energy. The loss from shadowing and blocking is usually a few percent. Refinement of this treatment adds corrections resulting in still smaller alterations. Computer runs that use each of the options will place limits upon the shadowing and blocking loss factors for a particular central-receiver design.

## II. Data Flow in HELIOS

The HELIOS Code is written as a series of five overlays as a means to conserve computer storage. The basic data flow in the main overlay (common to all overlays) is outlined in Figure 2. When the function of a block is fulfilled by a subroutine or by a program overlay, its name is included in parentheses. The emphasis in this report is upon the input data options (INDATA subroutine). A companion report<sup>1</sup> gives detailed explanations of the methods used. Figures 3 through 6 give flow diagrams for the programs that control each overlay. Part III of the user's guide provides diagrams and discussion for other routines.

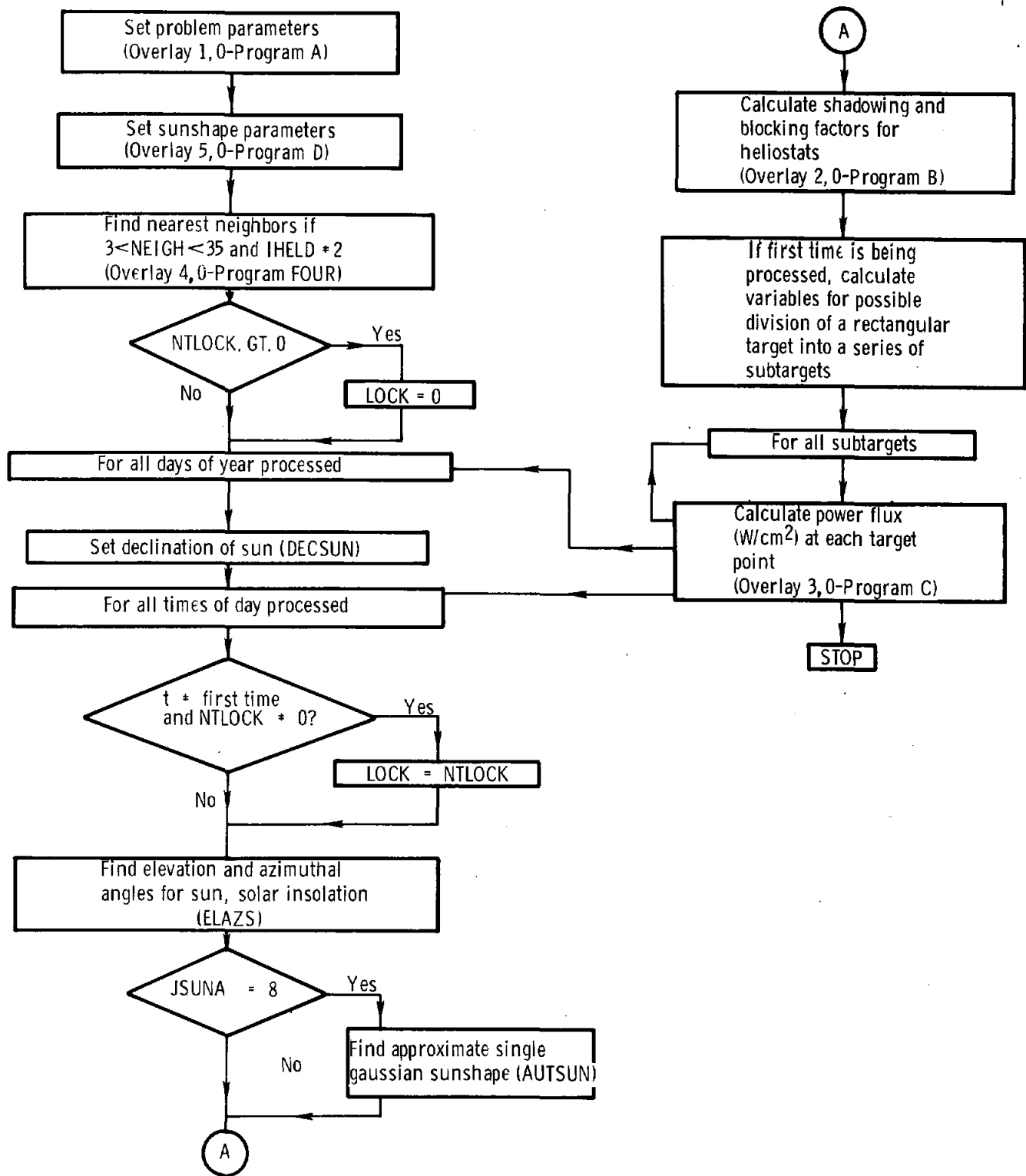


Figure 2. Basic Flow for the Main Overlay, HELIOS 0,0 (appropriate routine names are in parentheses)

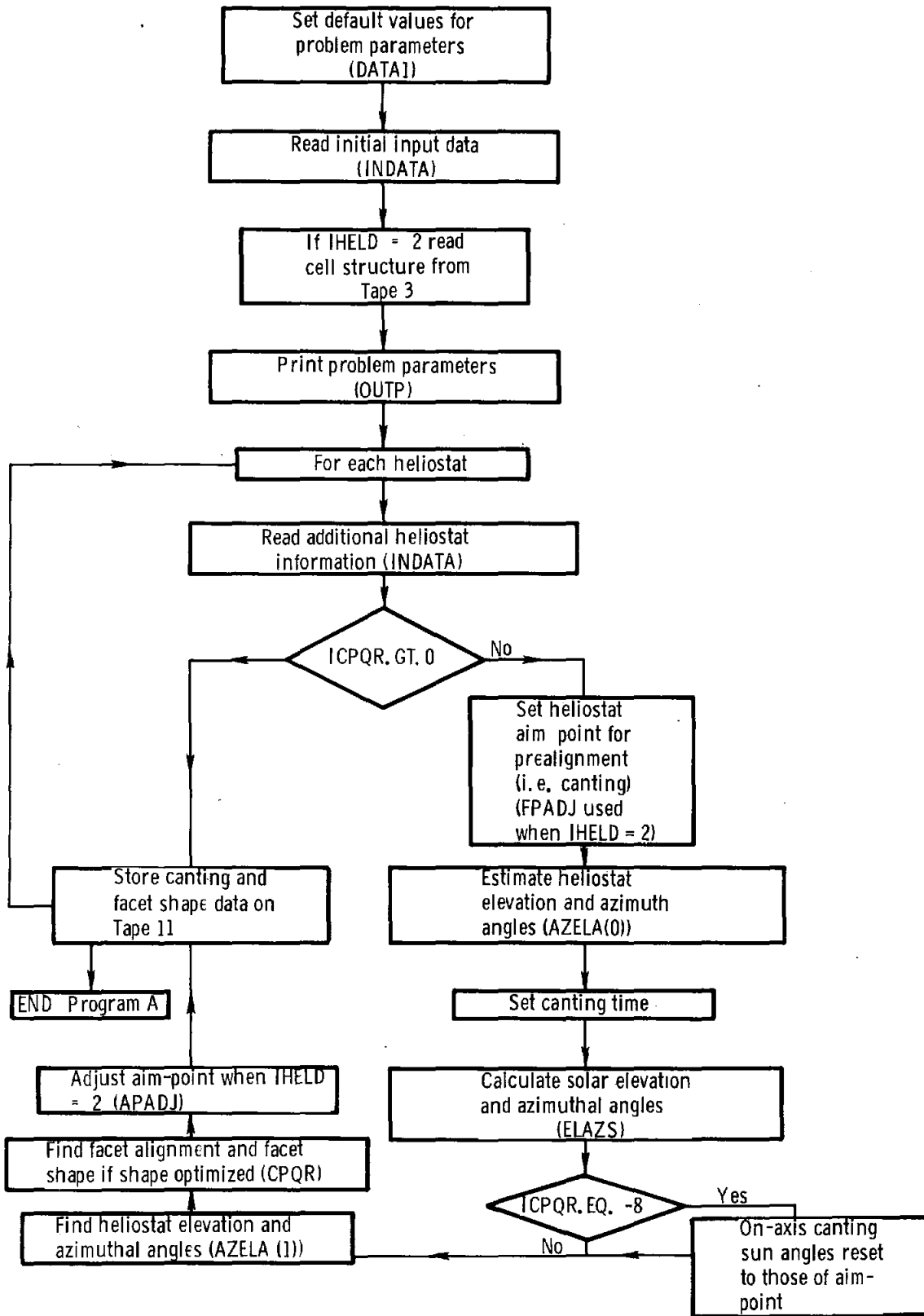


Figure 3. Flow Diagram for Overlay 1,0 — Program A

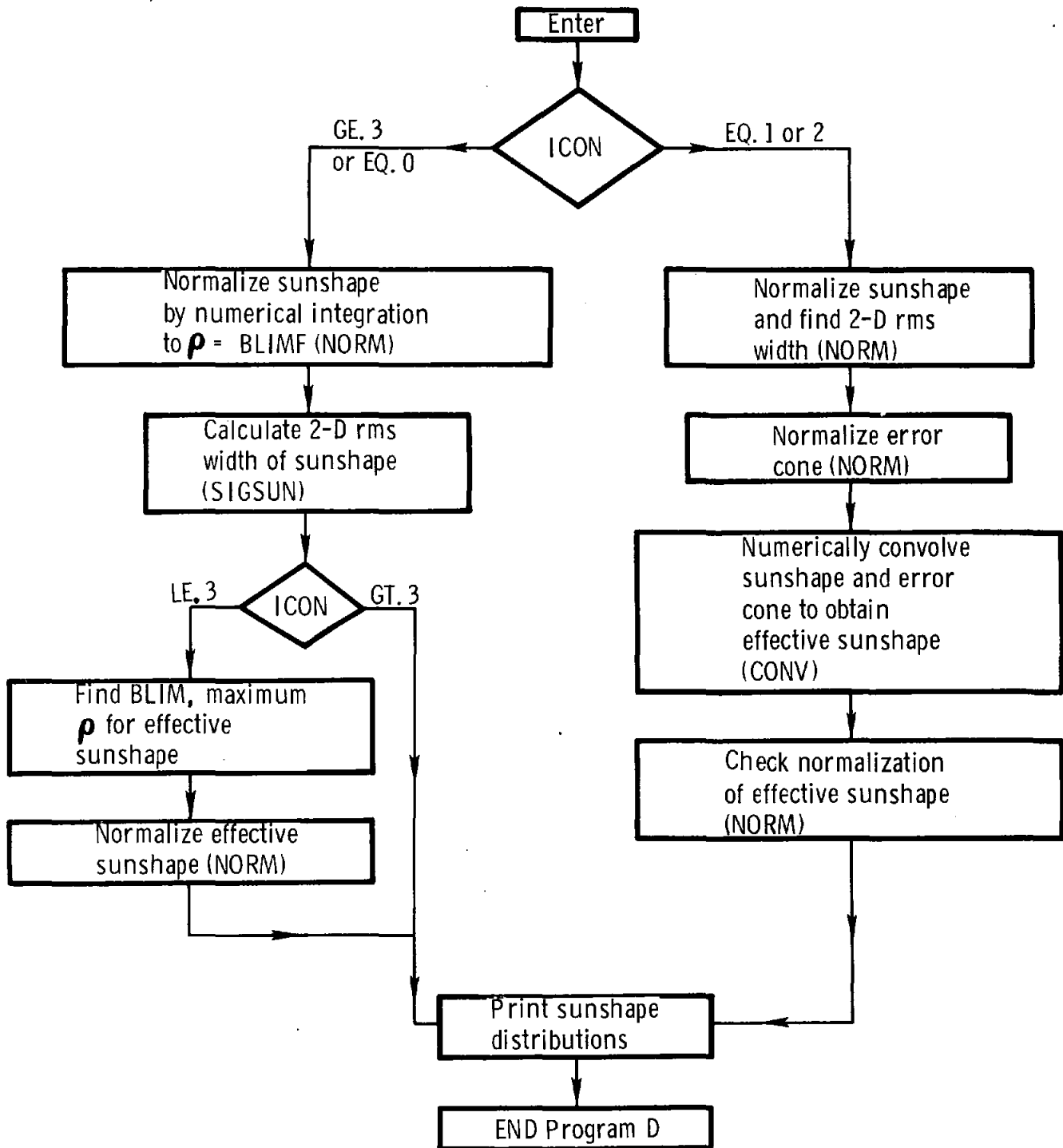


Figure 4. Flow Diagram for Overlay 5.0 — Program D

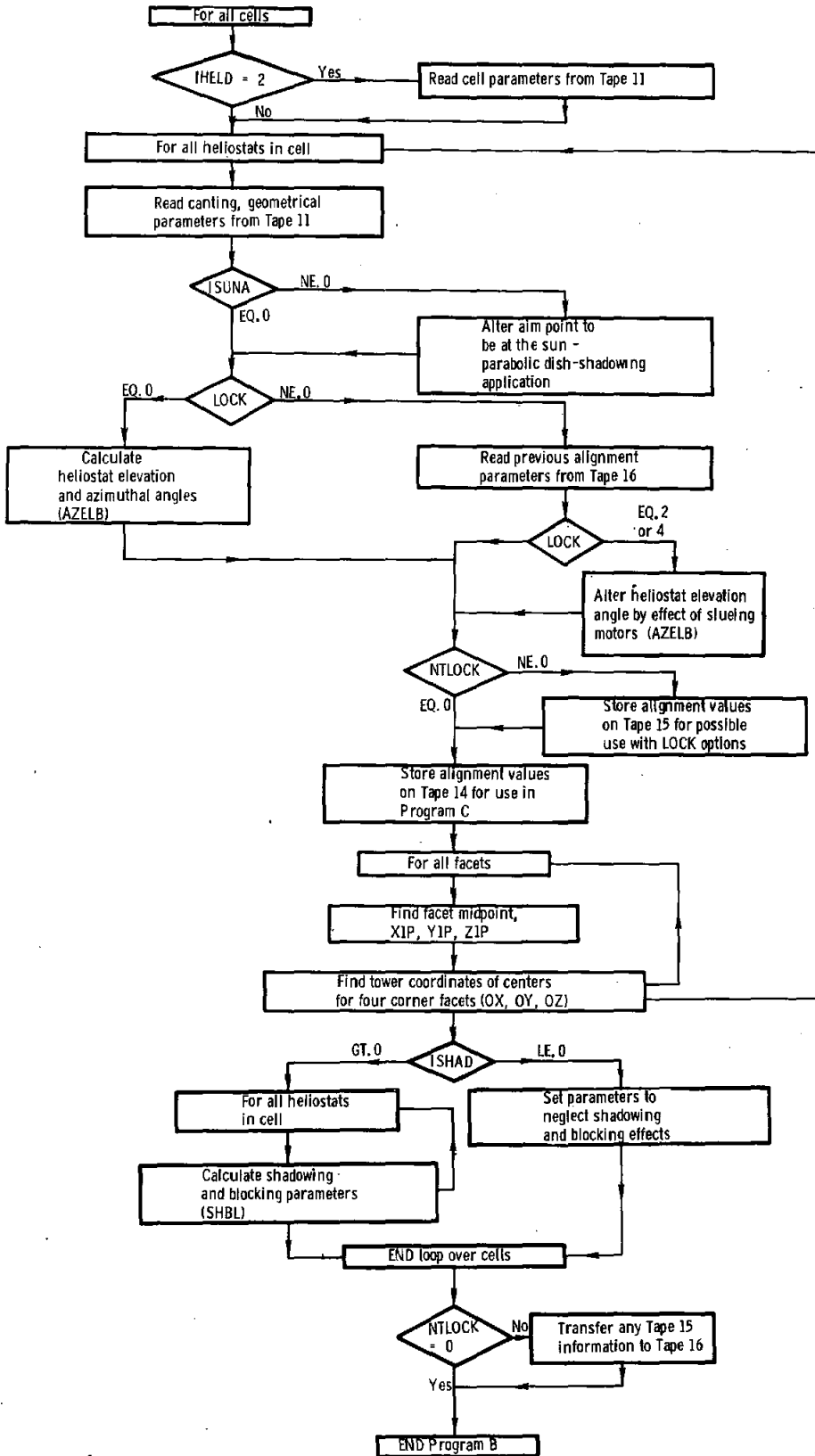


Figure 5. Flow Diagram for Overlay 2.0 — Program B

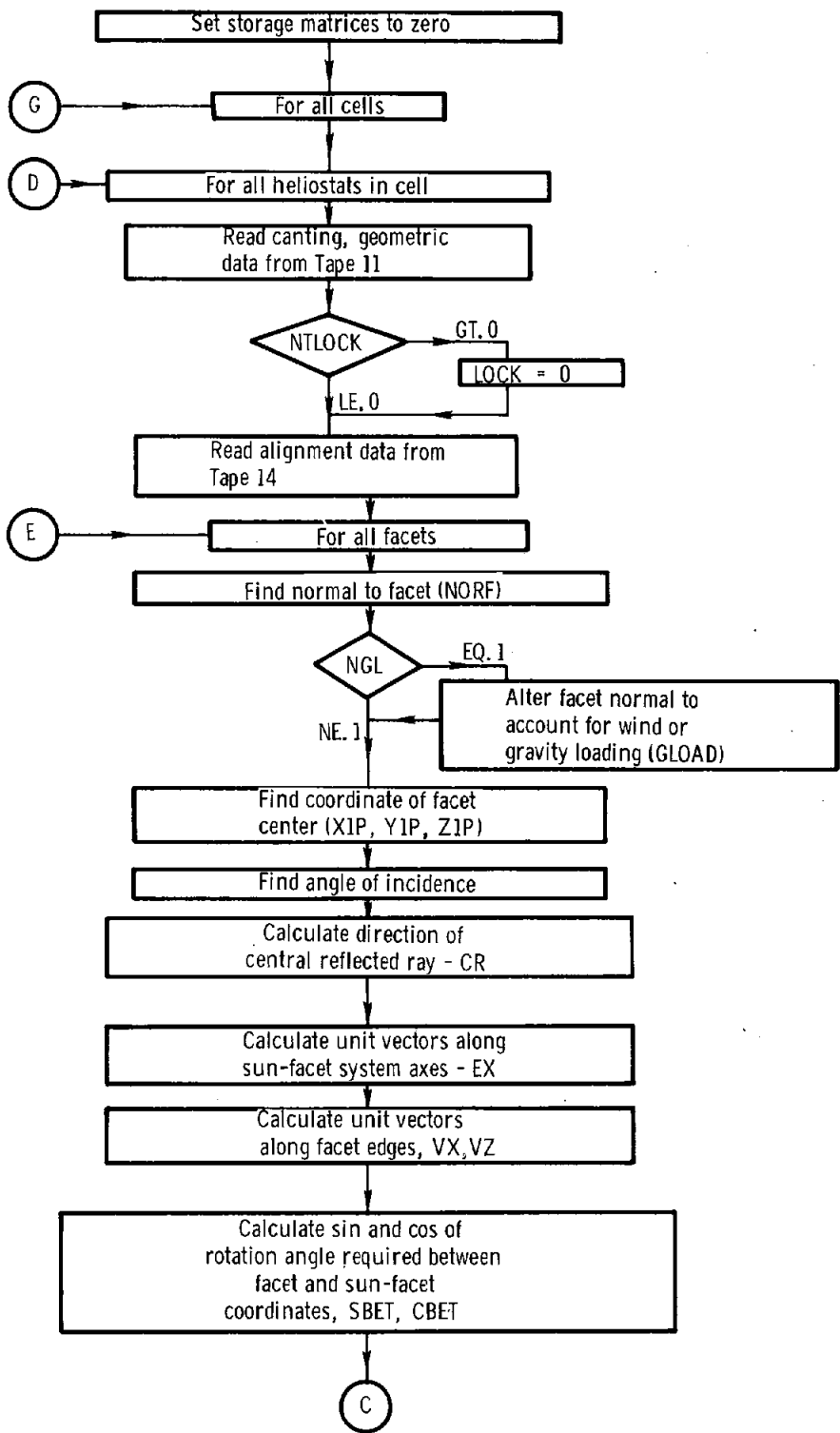


Figure 6. Flow Diagram for Overlay 3,0 — Program C

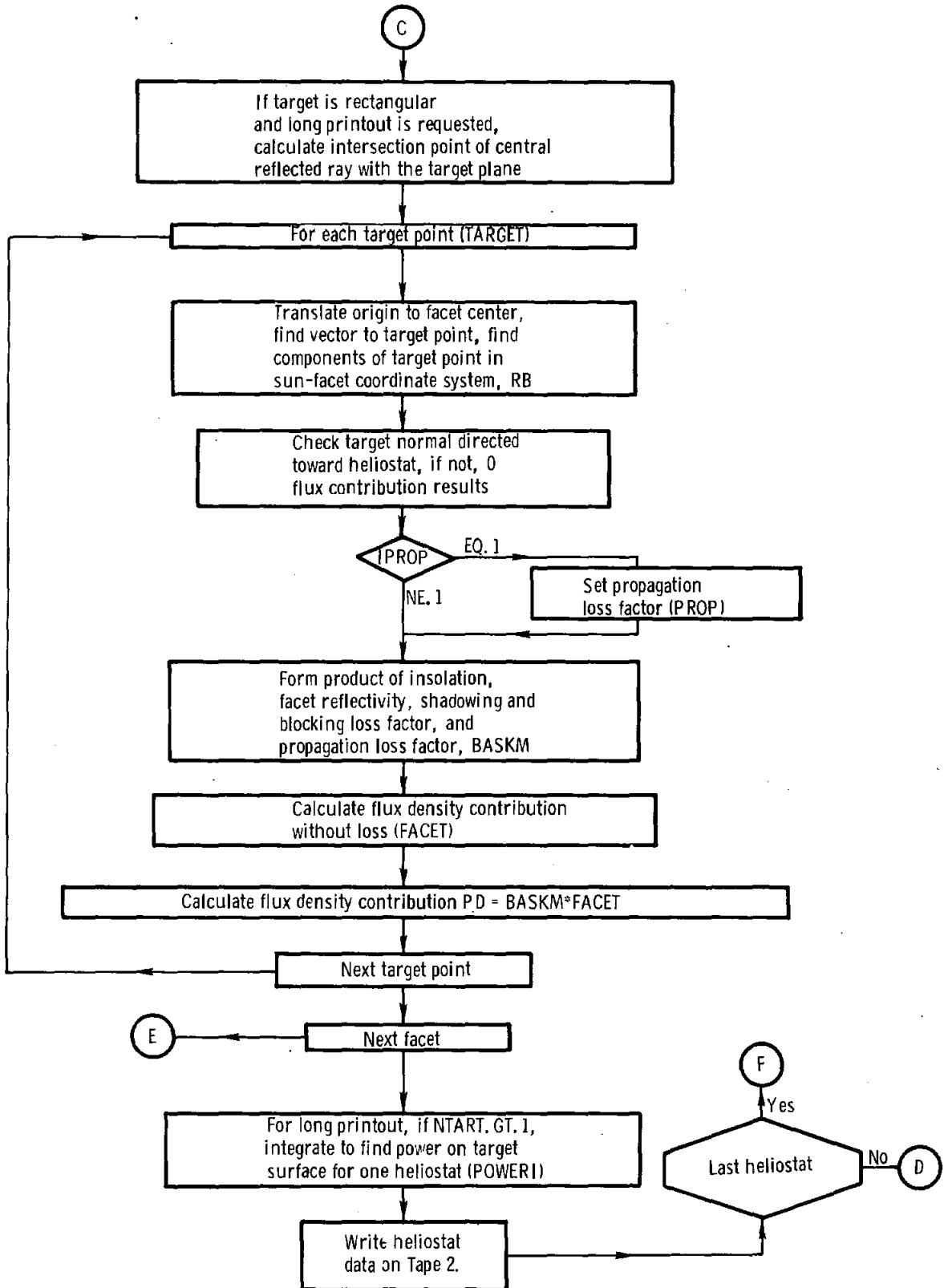


Figure 6. Continued

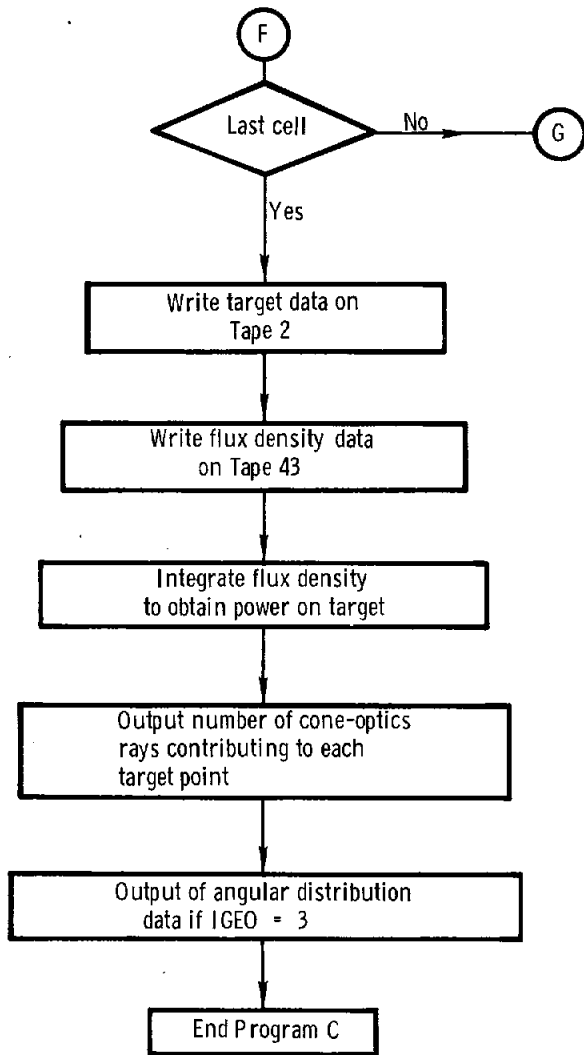


Figure 6. Concluded



### III. HELIOS Input

The HELIOS data are separated into seven divisions: problem and output type, sun parameter, receiver, facet, heliostat positioning, time, and atmospheric. Each division is characterized by a group number NGRUP as indicated in Table 1. As each new problem is encountered, new data need only be read in for groups with data differing from the previous problem. Hence, each group of data may be discussed separately from the other groups. The Code is initialized with default values for each input parameter. A comment card precedes each input data group in the input file to aid in identifying the variables. The comment is also transferred to the output file to record the groups where data alterations occur. Each group of data is now illustrated. Options associated with available choices for the variables are also noted.

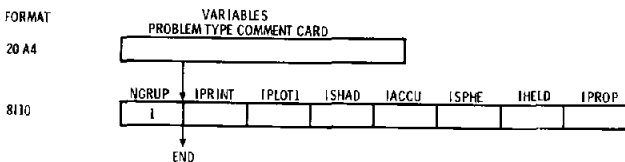
Table 1. Input Data Groups

Data Group	NGRUP	Discussion Page
Problem and Output	1	19
Sun Parameters	2	21
Receiver Parameters	3	26
Facet Parameters	4	30
Heliostat Parameters	5	33
Time Parameters	6	35
Atmospheric Parameters	7	36

This is the most important section for the user of HELIOS. It follows the organization of the INDATA subroutine where all input occurs. For understanding the capabilities of HELIOS and for easy adoption to similar types of problems, this subroutine should be studied by Code users. Appendix A gives input-data flow charts in a convenient form for listing data to process specific problems.

The discussion of input cards for each group starts with the input format, then lists the specific variables in order, and finally lists the options associated with available choices for the variables. The user is free to put any comments on Card 1 of each group. Copies of the Appendix A could serve as convenient forms for compiling specific problem data.

#### Group 1 Input Cards – Problem Type

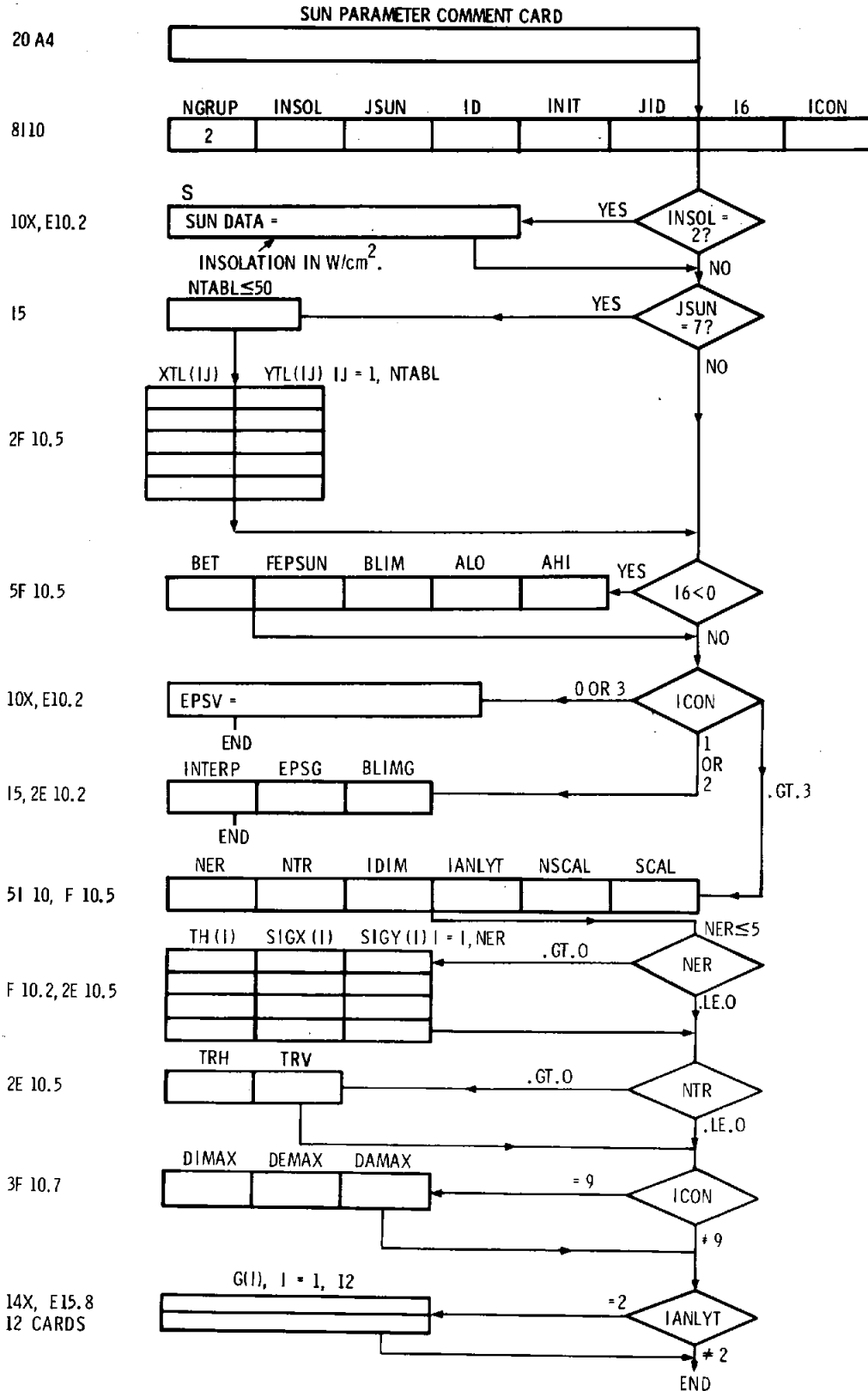


### Options

- NGRUP = 1 Index verifies the comment Card.
- IPRINT = 0 Index for short output. The printout includes the flux density ( $W/cm^2$ ) produced by all the heliostats at the grid of target points. The power intercepted by the mirrors and that incident upon the target are given. The facet area reduced by the angle-of-incidence effect and the area further reduced by shadowing and blocking effects are given. These data are given for each designated calculation time
- = 1 Index for intermediate output. The printout yields the above output variables for each heliostat in addition to the total. The loss factor caused by light propagation between facet and receiver is also given for each heliostat.
- = 2 Index for detailed output. It is especially useful for detailed examination of results for checking before a large computer run. It includes facet, heliostat, target point and alignment information, sun orientation, and detailed shadowing and blocking information including lists of the blocked (shadowed) and blocking (shadowing) heliostats. All the above output options include (1) a table describing the built-in model of atmospheric mass as a function of apparent elevation angle of the sun, (2) a table describing the built-in model of atmospheric refraction as a function of solar elevation angle, (3) brief descriptions of the input data groups, (4) tabular distributions of the sunshape, the error cone, and the effective sunshape, (5) tower coordinates of each target point and the components of the unit vector normal to the target surface at each point in the grid, and (6) a listing of the main problem parameters.
- = -1 Index for NOS (Network Operating System; i.e., an SNL time-sharing computer system) output. This option gives the IPRINT = 0 data in a slightly different format that is more convenient for NOS terminal output.

- IPLOT1 = 40 Plotting is to occur. At present, that value is needed if a shadowing and blocking data tape is to be generated.
- = 0 No plotting data are stored on Tape 40.
- ISHAD = 0 Shadowing and blocking are neglected. No shadowing and blocking tape is generated.
- = 1 Value >0 produces tape output for later shadowing and blocking calculation or plotting. One indicates that (1) when a heliostat is blocked by more than one heliostat, its blocked areas are added; (2) when a heliostat is shadowed by more than one heliostat or by the tower, its shadowed areas are added; and (3) when heliostats are both shadowed and blocked, the larger of the two areas is taken as the ineffective portion of the heliostat. The ineffective portion is limited by the total projected area.
- = 2 Value indicates that (1) blocked areas are assumed to overlap when blocking occurs by more than one heliostat; (2) shadowed areas are assumed to overlap when shadowing occurs by more than one heliostat or tower, and (3) when heliostats are both blocked and shadowed, the larger of the two areas is taken as the ineffective portion of the heliostat. This option is useful for upper-limit safety calculations.
- IACCU = 0 No flux-density calculation.
- = 1 Detailed calculation of flux density for each facet. The IOPT = 5 (Group 4 discussion) can be used to speed the calculation with some sacrifice of accuracy.
- ISPHE = 0 Index has lost generality because of alterations in the HELIOS Code. The 0 index is now useful only with IHELD = 0. In that case subsequent heliostats can be treated with alterations in the Group 5 variables NHELI, ICPQR, LOCK, I5, NTLOCK, I7, HE, HN, HZ, HL1, HL2, PN, QN, and RN. The initial value of NHEST in Group 5 gives the number of heliostat designs and positions to be treated. In studies of design variation using this approach, the summary matrices (giving the summation of results for all heliostats) may be of little use. Individual heliostat results will be of interest.
- = 1 Index indicates that a series of heliostat positions are to be processed. The heliostat number (NHELI in Group 5 data), the heliostat position, its aim-point, and its prealignment point can be defined for each heliostat calculation.
- IHELD = 0 Index for heliostat distribution indicates that the default distribution of heliostat positions (as for the CRTF) is sufficient.
- = 1 Index indicates new heliostat field layout and design parameters are to be read when Group 5 data appear.
- = 2 Index indicates new heliostat-field layout and design parameters are to be read (in order of cells) from Tape 3 (rather than input file) when Group 5 data appear. In present form, heliostat parameters are read in a series of unformatted records, each containing NHELI, HE, HN, HZ, and NC (cell number) for a heliostat. In this option the number of heliostats may exceed 559. Prealignment and aim-points are obtained from Subroutines FPADJ and APADJ rather than from matrices XFOC, YFOC, ZFOC, and XPOT, YPOT, ZPOT in Group 3 data.
- IPROP = 0 Index indicates propagation loss between mirror and target is neglected.
- = 1 Propagation loss is included based upon the model chosen by the Group 7 variable LFORM.

Group 2 Input Cards – Sun Parameters



## Options

- NGRUP = 2 Index verifies that this is Group 2 data.
- INSOL = 2 INSOL = 2 indicates that the sun insolation (in W/cm<sup>2</sup>) is to be read on the following card (i.e., the variable S).
- ≠ 2 Index indicates that the sun insolation is to be determined by the HELIOS Code.
- JSUN = 1 Gaussian sunshape with its peak matching the intensity of a uniform disk is chosen.
- = 2 Gaussian sunshape with its root-mean-square (rms) width matched to that of the sun is chosen.
- = 3 Uniform disk is chosen as the sunshape. The radius of the disk is controlled by the input variable FEPSUN that is discussed along with parameter I6. If desired, the user can adjust FEPSUN to match the 1.5% variation of the solar-disk half-angle with day of the year.  
 $1/2 \text{ angle} = 4.66 \text{ mrad} [1. + 0.015 \cos(0.986(\text{Day}-1))]^3$
- = 4 Sunshape option indicates a Kuiper distribution<sup>1</sup> for the sunshape, including limb darkening appropriate for wavelength 0.5 μm. This approximation may include the default parameter BET = 2.2 (if I6.GE.0).
- = 5 Sunshape is specified by user; Subroutine USERA must be altered.
- = 6 Sunshape is specified by user; Subroutine USERB must be altered.
- = 7 Sunshape is found by linear interpolation from table of values. Values are usually found by numerical fit to experimental measurements. When JSUN = 7, the number of values (NTABL) is read next (I5), followed by NTABL cards with values of tan α (XTL(I)) and the normalized intensity (YTL(I)).
- = 8 Gaussian sunshape is chosen with its rms width matched to that of the sun. The width is consistent with the solar insolation calculated for each time processed. JSUN is reset and will appear as one in the output.
- JSUN, ID, JID, AND I6 are all ignored when IANLYT ≥ 2.
- ID = 1 Cosine curve factor is used for round-off of sun's edge.  $1/2 (1. + \cos(\pi(\tan \alpha - \text{ALO})/(\text{AHI}-\text{ALO})))$  for  $\text{AHI} \geq \tan \alpha \geq \text{ALO}$ , and 0 for  $\tan \alpha > \text{AHI}$ .
- = 2 Gaussian curve factor is used for roundoff of sun's edge.  $\text{EXP}(-1/2((\tan \alpha - \text{ALO}/\text{AHI})^2))$  for  $\tan \alpha \geq \text{ALO}$ .
- = 3 Linear decay to 0 of intensity at the sun edge is used from  $\tan \alpha = \text{ALO}$  to AHI.
- = 4 Abrupt drop of intensity occurs from the uniform disk value to 0 at the edge.
- = 5 Abrupt drop of intensity to 0 occurs at  $\tan \alpha = \text{AHI}$ .
- = 6 Exponential drop of intensity,  $\text{EXP}(-(\tan \alpha - \text{ALO})/\text{AHI})$  begins at  $\tan \alpha = \text{ALO}$  to describe the sun's edge.
- INIT = 1 Initialization parameter is no longer used. Any value suffices.
- JID = 1 Sunshape in the limb ( $\text{ALO} \leq \tan \alpha$ ) is evaluated by multiplying the value at  $\tan \alpha$  by the smoothdown function determined by ID. This choice gives greater limb darkening for the sun.
- = 2 Sunshape in the limb ( $\text{ALO} \leq \tan \alpha$ ) is evaluated by multiplying the value at ALO by the smoothdown function determined by ID.
- I6 = 2 Value ≥ 0 indicates that the default values for sunshape parameters are to be used.
- < 0 Sunshape parameters BET, FEPSUN, BLIM, ALO, and AHI must be read. BET is the beta factor in the Kuiper sunshape. FEPSUN is the factor by which the sun's half-angle (4.64525 mrad) should be increased. After multiplication the tangent function converts to the width variable EP-SUN (DELF in common block CFF). BLIM is the tan α beyond which the solar intensity is 0; i.e., the limb edge. The rms width of the sunshape is often sensitive to the choice of BLIM. The other variables are explained with the ID parameter.

- ICON = 1 Convolution of the sunshape with the error cone may be done several ways. Index 1 indicates that the convolution is performed numerically, using fast Fourier transforms. The error cone is restricted to azimuthal symmetry, where the magnitude is specified by the angle from the central ray for the distribution.
- = 2 Convolution is performed analytically, assuming that each distribution is an azimuthally symmetric gaussian. An azimuthally symmetric sunshape is sometimes referred to as a one-dimensional (1-D) shape since the distribution is described by one variable; i.e., the angle from the central solar ray. The gaussian representing the sunshape has the same rms width as the sunshape used as input.
- = 3 or 0 Analytical convolution of azimuthally symmetric error cone with sunshape occurs only if the sunshape is gaussian. Otherwise errors are taken as negligible. The dispersion (EPSV) defining the error cone is required as input. As EPSV is altered. The user may also wish to change BLIM. Judgment is made by inspecting printout of the effective sunshape.

ICON.LT.4 The convolution is performed once per problem, with the original azimuthally symmetric treatment to give the effective sunshape. The error cones are input in the reflected-ray reference system.

ICON.GE.4 New options allow separate input for various contributions to the error cone. These options result in 1-D or two-dimensional (2-D) effective sunshapes. ICON also controls the frequency of evaluation of a new effective sunshape. The 2-D effects are treated in Chapter 5 of Reference 1. In general, the effective sunshape varies with the rotation angle to transform from the heliostat coordinate system to the sun-concentrator system, with the elevation angle of the heliostat, and with the angle of incidence at the reflector.

- ICON = 4 New convolution occurs only once per computer run. The effective sunshape will be appropriate for the first subfacet (integration element) on the first facet of the first heliostat treated at the first time specified by the HELIOS data.
- = 5 A new convolution occurs for each new time processed.
- = 6 A new convolution occurs for each heliostat at each new time processed.
- = 7 A new convolution is obtained for each facet on each heliostat at each new time processed.
- = 8 A new convolution is obtained for each subfacet of every facet treated by ICON = 7. Such detail might be desired for treatment of a parabolic dish (1 facet per heliostat) where the angle of incidence could vary significantly over the surface. The option also might be used to determine appropriate values of DIMAX, DEMAX, or DAMAX for use with ICON = 9.
- = 9 A new convolution is obtained whenever the angle of incidence changes by more than DIMAX (in radians), or the angle alpha required to rotate from the heliostat coordinate system to the sun-concentrator coordinate system changes by more than DAMAX (in radians) from its value when the previous convolution was made, or whenever the heliostat elevation angle changes by more than DEMAX (in radians) from its value when the previous convolution was done.

When ICON = 1 or 2, the error distribution is specified in a simplified manner. The new variables INTERP, EPSG, and BLIMG are then required.

In association with the choice ICON = 9, the three variables DIMAX, DEMAX, and DAMAX (in radians) must be defined by the input data.

- INTERP = 1 Linear interpolation is used between tabular points giving the effective sunshape distribution.

= 2 Cubic spline interpolation is used between tabular points giving the effective sunshape distribution.

EPSC

Half-angle (dispersion) of the error distribution is EPSC. In actual measurements, this variable may not be well-known. Hence, variation of results with EPSC is of interest for comparison with experimental data. The half-angle of the solar disk as seen from each facet is the FEPSUN variable, noted earlier, times the default value of the solar half-angle. This default value is EPSCW = 0.0046525 rad (i.e., for uniform disk distribution). Choosing ICON ≤ 3 gives an error cone of the form  $F(\rho) = (2\pi\sigma^2)^{-1} \exp(-\rho^2/2\sigma^2) N$  for  $\rho \leq$  BLIMG and EPSC =  $\sigma$ . The function is normalized by choice of N such that

$$\int_0^{\text{BLIMG}} F(\rho) 2\pi\rho d\rho = 1.$$

For Large BLIMG the 2-D rms width is  $\sqrt{2} \sigma$ . The error cone is combined with the sunshape directly; thus it includes the factor  $\approx 2$  increase over slope error at small angles of incidence. Suppose the standard deviation of the mirror-normal slope error distribution (measured in a single plane containing the normal) is  $\sigma_s$ . Also assume that the standard deviation in the orthogonal direction is  $\sigma_s$  and that  $\sigma_s$  is sufficiently small that  $\tan \sigma_s = \sigma_s$ . The rms width of the 2-D distribution representing the surface normal is  $\langle \rho^2 \rangle = \langle x^2 \rangle + \langle y^2 \rangle$  or  $2 \sigma_s^2$ , giving an rms width  $\sqrt{2} \sigma_s$ . Multiplication by 2 approximates conversion to the reflected-ray reference system. Setting this rms width,  $2 \sqrt{2} \sigma_s$ , equal to the rms width of the error cone,  $\sqrt{2} \sigma$ , indicates EPSC =  $\sigma = 2 \sigma_s$  to approximate this error with ICON ≤ 3. This approach was used for the first comparison of field calculations by HELIOS and by MIRVAL.<sup>4</sup>

BLIMG = Parameter corresponds to the BLIM of the sun's intensity distribution. When ICON = 3, the distribution is

truncated at  $\tan \alpha =$  BLIM. BLIMG is required to determine the upper limit of  $\tan \alpha$  for the effective sunshape (EL in INDATA) when ICON = 1 or 2.

Earlier versions of HELIOS, where ICON ≤ 3, required several other parameters to define the error cone: NDIR, JSUNG, IDG, JIDG, BETG, ALOGG, AHIG, and EPLE. Experience indicated these variables were not altered often enough for inclusion. When ICON = 1 or 2 they are now internally defined by the Code. Matrix dimensions now require NDIR = 4. JSUNG is set to 2, signifying a gaussian error cone. IDG is set to 3, indicating linear decay of the error cone between ALOGG and AHIG (i.e., when combined with JIDG = 1). The JIDG is set to 1, BETG is set to zero and is not used in these options. ALOGG is defined as BLIMG - 0.001. AHIG is set to BLIMG. Lastly, EPLE is set to 0 and is not used in these options.

In the more detailed treatments where ICON > 3, heliostat errors are divided into two categories: concentrator and sun-tracking. These separate categories are convenient because of the difference in the invariant descriptions of these two types of errors. Concentrator errors can be combined in the concentrator system to obtain a description that is independent of heliostat orientation. The sun-tracking errors are specified with respect to the individual tracking axes.

NER = Number of concentrator errors introduced in the heliostat coordinate system.  $0 \leq \text{NER} \leq 5$

NTR = 0 Tracking errors neglected.  
= 1 Tracking errors included.

IDIM = 1 or 2 The number of dimensions in the effective sunshape treatment.

IANLYT = 0 Numerical convolutions used.  
= 1 Analytical convolutions occur with sunshape represented as a gaussian distribution with the same rms width as for the input sunshape.  
≥ 2 Analytical convolutions occur with the sunshape represented as a sum of gaussian distributions. The form of the representation is

$$\sum_{i=1}^3 G_i \exp(-G_{i+1} \rho^2) [1 - G_{i+2} \exp(-G_{i+3} \rho^2)]$$

Where  $j = (i-1)*4 + 1$ . Allowed values of IANLYT here are 2, 9, 7, 10, 6, 16. Value 2 indicates the G values are read in. The other values indicate analytic fits of the corresponding Data Set in the LBL set of standard sunshape profiles.<sup>1</sup> The data set numbers are in order of increasing rms width. This option is particularly useful for saving computer time when convolutions are performed often, or when a sunshape is to be estimated conveniently.

- NSCAL = 0 Analytic sunshape is not scaled.  
 ≠ 0 Analytic sunshape parameters are scaled by the factor SCAL to adjust sunshape for differing atmospheric parameters.
- SCAL = This factor gives the ratio of the new normalized sunshape peak to the peak for the old shape. The shape is determined by a sum of gaussians ( $IANLYT \geq 2$ ) with coefficients altered in the SUNPAR subroutine. The factor is used when NSCAL.NE.0.

### Concentrator Errors

When  $NER = 0$ , no concentrator errors are treated in HELIOS. For  $NER > 0$ , these errors might include

reflectance-cone (nonspecular), slope (mirror waviness), large scale curvature variation, and perhaps canting errors. Each of the error distributions is described by an elliptic-normal distribution specified by an angle  $TH(I)$  and two standard deviations  $SIGX(I)$  and  $SIGY(I)$ .  $TH(I)$  is the angle in degrees from the  $U1$  (horizontal axis of the heliostat system) to the principal axis of the elliptic-normal distribution corresponding to the standard deviation  $SIGX(I)$ ; the positive direction is counterclockwise as seen facing the concentrator. The standard deviations are tangents of angles. The three values  $TH(I)$ ,  $SIGX(I)$ , and  $SIGY(I)$  define a given contribution to the error in the normal to the surface of a reflecting mirror.

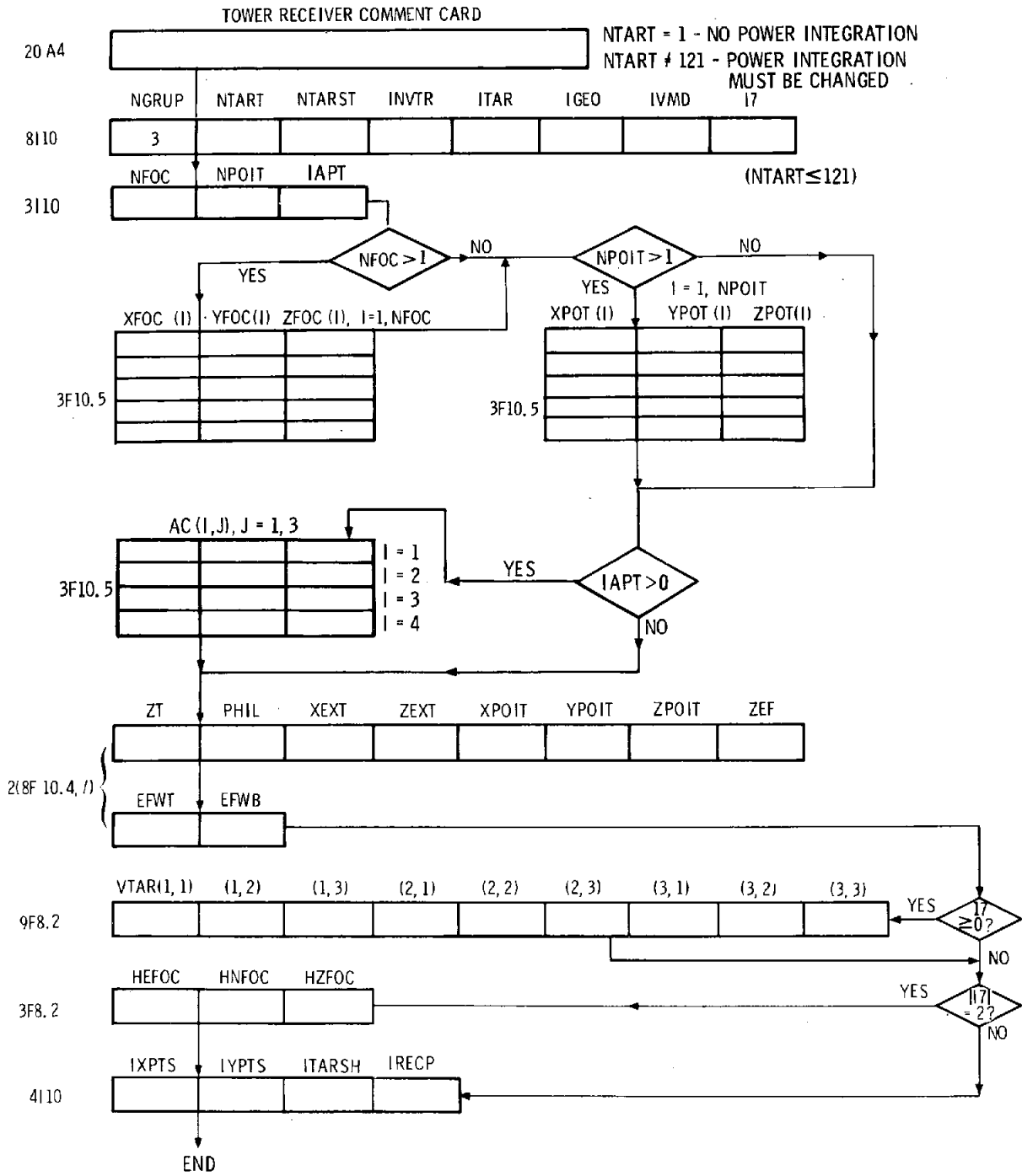
### Sun-Tracking Errors

When  $NTR = 1$ , the variables  $TRH$  and  $TRV$  are required. They are standard deviations (tangents of angles) of 1-D normal distributions describing the accuracy of tracking along the horizontal elevation axis ( $TRH$ ) and the vertical azimuthal tracking axis ( $TRV$ ).

### Bounding Calculations

An upper limit to the collected power may be obtained by inserting zero errors and a narrow sunshape. The user is warned that a single gaussian sunshape ( $JSUN = 1$  or  $2$ ) gives a peaked distribution that will grossly overestimate the peak flux density. The default sunshape ( $JSUN = 4$ ,  $ID = 6$ ,  $JID = 2$ ,  $I6 = 1$ ,  $ICON = 3$ ) is a better optimistic sunshape to use.

Group 3 Input Cards -- Receiver Parameters





## Options

- NGRUP = 3 Index verifies that we have Group 3 data.
- NTART = 121 Variable gives the number of target points in the target mesh. Dimension statements restrict values to  $\leq 121$ .
- NTARST = 59 Parameter gives the target point index at which printing may start to give results for individual facets. At present, detailed printout occurs for only three target points.
- INVTR = 2 Interval between target point indices at which individual facet results are printed is given as 2. These choices make the center print-point the center of the target mesh when standard target meshes are chosen.
- ITAR = 1 ITAR  $\leq 0$  automatically sets the center of the target mesh to the coordinates at which the heliostat is aimed. Here, ITAR  $> 0$ , so the coordinates read in for the purpose give the center of the target mesh.
- IGEO = 0 Power-per-unit area is found for points on the target surface.
- = 1 Power-per-unit area arriving at each target point is calculated normal to the central reflected ray for each individual facet. In general, this normal will not be orthogonal to the target surface. The option may be useful for finding upper bounds to the power received on selected (perhaps oddly shaped) targets.
- = 2 In addition to the IGEO = 0 output, the three components of the energy flux are given at each of the target points in the grid.
- = 3 In addition to the IGEO = 0 output, the angular distribution of flux density is given at each target point. Because of added storage requirements and infrequent use, program alterations are required.

In Program C, the brightness matrix (B) in common block BCOM must be altered to contain more than one tabulation bin for polar and azimuthal angle. For example, B (121, 15, 60) specifies 15 polar angle bins and 60 azimuthal angle bins at each of the 121 target points. Use with a CDC 7600 may require a

LEVEL 2, B statement to assign the matrix to extended-core storage. In Subroutine DATA1 the number of (cosine) polar-angle intervals (IMAX), the number of azimuthal-angle intervals (JMAX), the width of each interval (DTHETA, DPHI), and upper and lower limits for tabulation must be adjusted for the problem of interest. When the level statement is used, the job card may need to request extended core storage; i.e., EC400 on the CDC 7600 system at SNLA. ITARSH = 7 is not allowed when IGEO = 3. Output can be large when maximum allowable numbers are chosen for NTART, IMAX, JMAX. Six sets of 15 lines (15 polar angles) are required to print results for 60 azimuthal angles. This is about two pages of output for each of 121 target points. The calculation for one target point proceeds more quickly and produces a reasonable amount of output.

- IVMD = 1 IVMD indicates the general direction of the normal to the target surface when the target surface is flat. The value 1 indicates that the target faces north. Other values are indicated below. The direction must be specified well enough for the inner product of the actual normal and the specified direction to be positive. IVMD is not used when ITARSH = 3 or 4. It is of no consequence when IGEO = 1.
- = 2 Northeast
- = 3 East
- = 4 Southeast
- = 5 South
- = 6 Southwest
- = 7 West
- = 8 Northwest
- = 9 Downward
- = 10 Upward
- I7 = 1 I7  $\geq 0$  is used to direct the program to read in three vectors that specify the target orientation, VTAR (3,3).
- < 0 Value indicates that the target orientation is not needed (as when IGEO = 1 or NTART = 1). If I7 = 2, the coordinates of the point at which the heliostats are focused at prealignment time are read in after the following VTAR card.
- NFOC = NFOC gives the number of facet prealignment points or canting conditions in the heliostat-field design.

NFOC  $\leq 20$ . More points are available when IHELD (Group 1 data) = 2.

NPOIT = NPOIT gives the number of aim-points in the heliostat field. Multiple aim points are used to spread the energy more evenly over the target aperture. NPOIT  $\leq 222$ . More points are available when IHELD (Group 1 data) = 2.

NPOIT = -1 Adjusts the aim-point for each heliostat to be at the sun. This option has been used to estimate shadowing for a series of parabolic-dish collectors.

IAPT = 0 Receiver is not a cavity receiver.  
 = 1 Receiver is a cavity receiver. Solar rays are required to enter a rectangular aperture before they can strike the target. The test occurs in Subroutine APERT.  
 = 2 The aperture is circular.  
 = 3 Rays are tested in Subroutine APERT and excluded if they enter a user-defined volume. The IAPT = 1, 2, or 3 options are not now operational with triangular-shaped facets (KORD = 5).

XFOC(I) = For I = 1 to NFOC, these data are the  
 YFOC(I) = tower coordinates of each facet prea-  
 ZFOC(I) = lignment point. When NFOC = 1, the input occurs by means of the HEFOC, HNFOC, and HZFOC input later.

XPOT(I) = For I = 1 to NPOIT, these data are the  
 YPOT(I) = tower coordinates of each aim-point  
 ZPOT(I) = used. When NPOIT = 1, the aim-point is inserted by means of the XPOIT, YPOIT, ZPOIT noted later.

AC(I,J), J = 1, 3 = X, Y, Z tower coordinates of corner I in the aperture to the receiver. The corners are labeled clockwise by an observer facing the aperture from the front with the first corner being the upper left. In the case of a circular aperture, the four corners are those of the inscribed square with two horizontal edges.

ZT = ZT gives the altitude of the center of the tower peak in metres.

PHIL = PHIL gives the north latitude for the tower position in degrees.

XEXT = XEXT gives the horizontal extent of the target surface in metres for a flat target and in radians for spherical or cylindrical surfaces. At present, cylindrical surfaces are restricted to those with vertical axes.

ZEXT = ZEXT gives the extent of the target surface orthogonal to XEXT. ZEXT is in metres for flat or cylindrical targets and in radians for a spherical target surface.

XPOIT = All three coordinates specify the  
 YPOIT = tower coordinates of the aim-point  
 ZPOIT = for heliostats when NPOIT = 1. They also specify the center of the target mesh when ITAR = 0.

ZEF = These three variables give the  
 EFWT = effective height and effective  
 EFWB = radii at the top and bottom of the tower. These dimensions (in metres) are used in the shadowing calculation.

VTAR =  
 In the case of a flat target, (VTAR(1,I), I = 1,3) (VTAR(2,I), I = 1,3), and (VTAR(3,I), I = 1,3) are the coordinates (in metres) of three points in the target plane. The three points must not be colinear, since vector products are used to determine the target plane and its normal. The first vector specifies the center of the target mesh. Some may desire target coordinates that increase from left to right as you face the target. This will not always be the case. A north-facing target, for example, will have X increasing from west to east in agreement with the tower coordinates. An attempt has been made to print flux densities in the orientation seen by an observer facing the target.

For a spherical target surface, XEXT and ZEXT are the azimuthal- and polar-angle intervals to be spanned (in radians). (VTAR(1,I), I = 1,3) gives the tower coordinates of the center of curvature of the spherical mesh when ITAR > 0. The aim-point (XPOIT, YPOIT, ZPOIT) is the center of curvature when ITAR  $\leq 0$ . The center of curvature is referred to as the mesh origin. VTAR(2,1) is the distance from the mesh origin to the spherical surface. (VTAR(2,2) is the polar angle of the center of the target mesh measured from the vertical at the mesh origin. (VTAR(2,3) is the azimuthal angle of the center of the target mesh, measured from the east with the positive direction toward the north as viewed from the mesh origin. The vector (VTAR(3,I), I = 1,3) is not required as input; any values suffice.

A cylindrical target surface requires new meaning for the VTAR vectors. XEXT is, again, the azimuthal angle to be spanned. ZEXT is the vertical length to be spanned by the target. VTAR(2,1) is the horizontal distance from the mesh origin to the cylindrical surface. VTAR(2,3) is the azimuthal angle of the center of the target mesh as viewed from the mesh origin. (VTAR(1,I), I = 1,3) gives the coordinates of the mesh origin.

If  $|I7| = 2$ , data must be furnished to define the coordinates of the point at which the heliostat facets are prealigned (canted) at calibration time, HEFOC, HNFOC, and HZFOC (format 3F8.2). Otherwise, the top of the tower (0., 0., ZT) is used as the point of focus. When NFOC > 1, the prealignment point for each heliostat is chosen from the appropriate XFOC(I), YFOC(I), ZFOC(I).

IXPTS = 11 Number of target points along a horizontal direction is 11.

IYPTS = 11 Number of target points in the second coordinate of the the 2-D target grid is 11. Choices other than IXPTS = 11 and IYPTS = 11 require changes in the plotting routines for three-dimensional (3-D) graphs of the distribution of power on the target if such a graph is desired. Other choices also require alteration of integration techniques used to determine the power (in watts) on the target surface.

- ITARSH = 0 Target surface is rectangular.  
 = 1 Target surface is spherical.  
 = 2 Target mesh is supplied by the user; Subroutine USERTG must be altered.  
 = 3 Target mesh is cylindrical with a vertical axis and outward-drawn normal.  
 = 4 Target mesh is cylindrical with a vertical axis and inward-drawn normal.  
 = 5 The target surface is square, centered at VTAR (1,I), I = 1,3 and oriented orthogonal to the central ray from the first heliostat processed. The target extents are given by  $0.01 * (\text{target-heliostat distance in metres}) * \text{VTAR}(2,1)$ . When this option is chosen, the heliostat data (NGRUP = 5) must come before the NGRUP = 3 input so the first heliostat position is known.  
 = 6 The target surface is flat and circular, centered at VTAR (1,I), I = 1,3 and

with its plane defined by the VTAR vectors as for ITARSH = 0. XEXT is the target radius, ZEXT is taken as  $2\pi$ .

= 7 The receiver itself is flat and rectangular. However, up to six reconcentrators are used to increase the collected power. IRECP gives the number of reconcentrator panels. The receiver itself is defined by the normal ITARSH = 0 variables. The reconcentrator coordinates and unit normal vectors are specified for each section by the user-supplied target subroutine (USERTG) that occurs in overlay (0,0). Subroutines BASKET and RARE must also be written to replace those provided. Reconcentrator reflectivity is set in FACET.

= 8,9,...,17 The target surface is flat and rectangular. The internal code variable NTARSH is altered from 1 to ITARSH - 7. The XEXT and ZEXT are each divided into NTARSH subtargets, separating the target into  $\text{NTARSH}^2$  smaller targets, each with up to 121 target points. These options allow division of the target surface into up to  $101 * 101$  separate points for improved resolution in the flux density pattern. ITARSH = 8 is equivalent to ITARSH = 0. ITARSH = 17 divides the target into 100 subtargets. After calculation of NTARSH, the Code resets ITARSH to 0. An example of how the division occurs is shown in Figure 7. As you face the target, note that the edges of Subtargets 1 and 4 coincide. Hence the target points along the bottom edge of Section 1 should have flux densities identical to those of the top edge of Section 4. HELIOS printout of the tower coordinates at the four corners of each subtarget also helps orient the subtargets relative to each other.

The compound-target option is expected to be applied mainly to one heliostat at a time, during heliostat evaluation. With ITARSH = 17, the 100 separate targets give 12,100 target points. Calculation time is increased considerably. Even with the shortest printout option, more than 100 pages

of printout occur (the flux-density distribution and power summary for each of the 100 subtargets). Hence, ITARSH should be chosen carefully.

IRECP = When ITARSH = 7 the number of reconcentrator sections is IRECP. Otherwise IRECP is ignored. If reconcentrators are used, the number of apertures is IRECP/2 for 2-D reconcentrators.  $IRECP \leq 6$ .

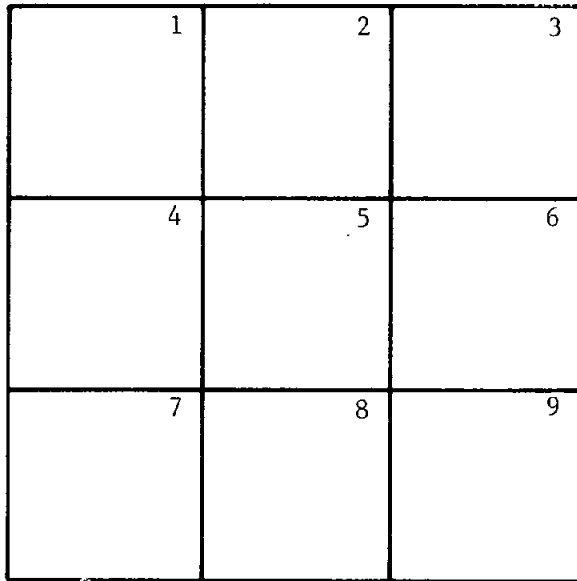


Figure 7. Target Subdivision for NTARSH = 3

The absorptance of the receiver is controlled by the Function ABSORP called by Subroutine PHI. The absorptance is set to 1 at the present time. An alternate form is given as comment cards in the ABSORP function listing. Some users may wish to alter that absorptance for special purposes.

### Options Group 4 Input Cards

NGRUP = 4NGRUP verifies that this is Group 4 data.

NFACET = Number of facets mounted upon each heliostat is NFACET ( $\leq 25$ ).

KORD = 1 Facets are square, with edge length = FLENG (m).  
 = 2 Facets are circular, with radius = FLENG (m).  
 = 3 Facets are rectangular with horizontal and orthogonal edge lengths = ELENX and ELENY, respectively. Integration over the facet is accomplished by dividing these lengths

into NX and NY segments and summing contributions from each element of area.

= 4 Facets are circular with a hole of radius RHOLE (m) at the center.  
 = 5 Facets are equilateral triangles with edge length ELENX. Each edge is divided into NX segments for integration over the mesh of elementary triangles. Either the bottom or top edge of the facets is assumed horizontal.

NSUBF = n Each square facet is divided into n x n sections for evaluation of the integral over the facet to obtain the facet's contribution to the power density received at one of the target points. Facets with unusually short focal lengths of unusually large dimensions require larger values of NSUBF. Each circular facet is radially divided into n sections with angular intervals chosen to be smaller than the radial interval. The variable is ignored for rectangular or triangular facets.

IOPT = 1 Parabolic facet shape. The facet shape really involves two concepts, the shape of the outer edge (circular, rectangular, triangular) controlled by the variable KORD, and the contour of the facet surface itself (spherical, parabolic, flat, etc...) controlled by the variable IOPT. The focal length is controlled by prealignment conditions.

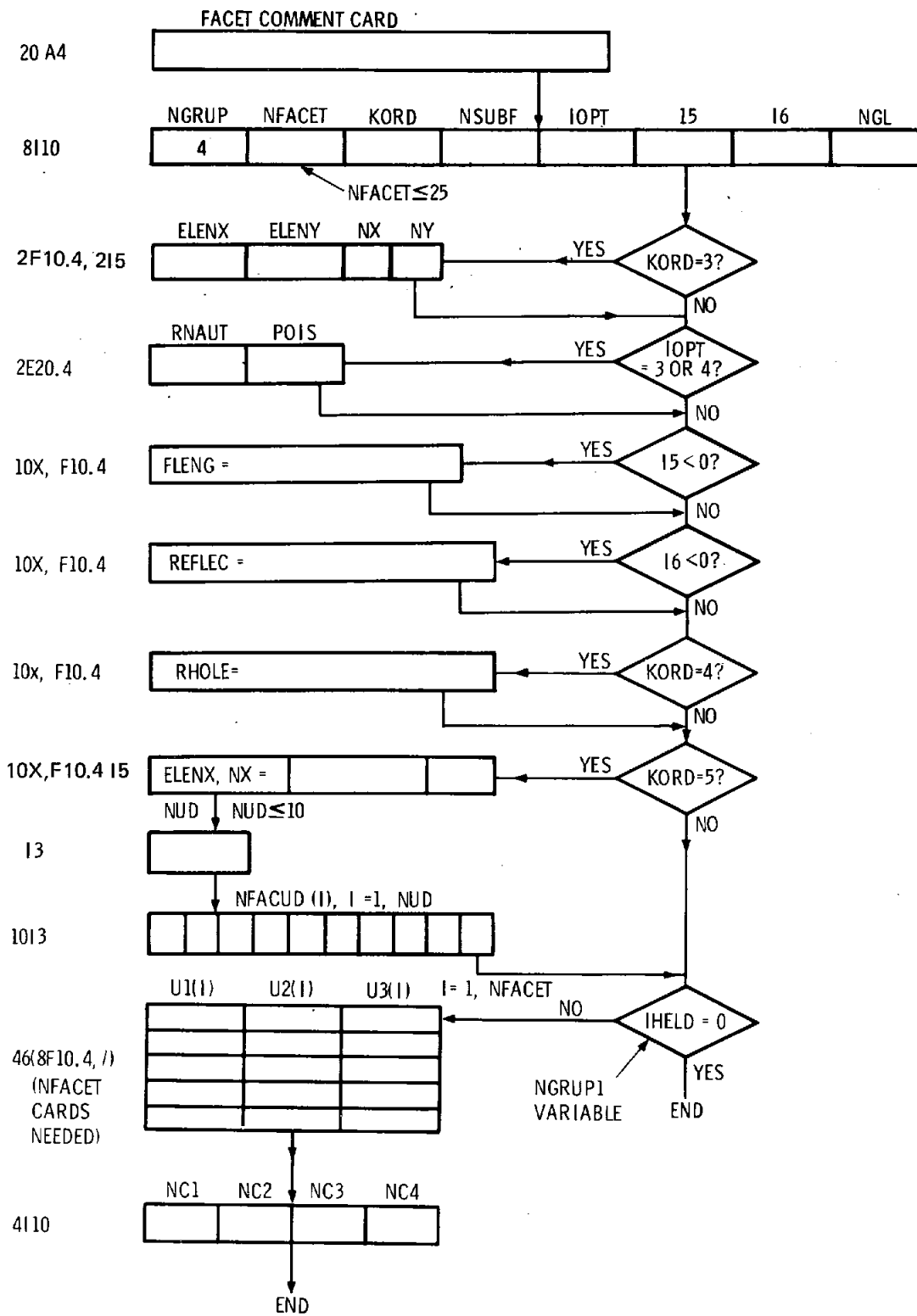
= 2 Flat facet contour.

= 3 Facet surface is determined from stress analysis of a square-glass facet supported by an outside ring and focused by pulling on the center by a uniform pressure applied to a circular region of radius RNAUT.

= 4 Facet surface is determined as in IOPT = 3 except that the center pull is exerted upon a ring of radius RNAUT. The IOPT = 3,4 options are referred to as Hoyle options.

Value IOPT = 3 or 4 would indicate reading variables RNAUT and POIS in 2E20.4 format. These variables are needed for IOPT = 3 or 4 if default values are not accepted. POIS

### Group 4 Input Cards – Facet Parameters



is Poisson's ratio for the facet material (default 0.3), and RNAUT is the radius of the focusing pull region or ring. At the CRTF IOPT = 4 and RNAUT = 0.2032 m.

= 5 Facet surface is continuously focusing; it is referred to as super-smart. This option is useful for speed (in effect, NSUBF = 1, which decreases running time by about a factor of NSUBF\*\*2) and for obtaining upper limits to the collected power.

= 6 Spherical facet shape. The radius of curvature is controlled by prealignment conditions.

= 7 Unit vector (VN(I), I = 1,3) normal to the facet is determined from the coordinates on the facet (RL(1), RL(2)) and a user-generated Subroutine USERVN. This option is useful when detailed measurements are available for a facet surface. The output then includes a listing of facet normals and facet coordinates for a series of points on a facet. If the facet shape varies with the heliostat chosen, the shape chosen for printout is that of the first heliostat. If heliostat data do not precede facet data, the default heliostat is chosen for this detailed facet-shape printout.

I5 = Value I5 < 0 would indicate that the length (in metres) of a facet side or the facet radius (FLENG) must be furnished. Otherwise, the default value (1.22 m) is used.

I6 = Value I6 < 0 would indicate that the facet reflectivity (REFLEC) must be read. The default value is 0.9. Subroutine REF may be altered for more detailed treatment of reflectivity.

NGL = 0 Gravity or wind-loading effect upon facet normal is neglected.

= 1 Gravity or wind-loading effect upon facet normal is included. Subroutine GLOAD provides the new facet normal (in the tower coordinate system) from the facet number, the heliostat elevation angle, the heliostat elevation angle at prealignment time, and the facet normal when loading is neglected. Tape 1 must be provided to

furnish facet normals as a function of elevation angle. Preparation of Tape 1 is discussed with the Subroutine GETNSF in Appendix A of Part III.

When IHELD = 1 (Group 1 data set), the facet positions must be specified in relation to the heliostat. These coordinates (in metres) are the variables U1, U2, U3, indicated roughly in Figure 8. The U3 axis completes the right-handed system. U3 is zero at  $x_1, y_1, z_1$  in Figure 9. Group 1 data must precede Group 4 so that IHELD has the proper value.

NC1, NC2, NC3, NC4 are the indices of the corner facets in clockwise order in Figure 8 (1, 5, 25, 21 are the default values appropriate for the CRTF).

When KORD = 5, NUD indicates the number of triangular facets that have their upper edge horizontal. NFACEUD (I), I = 1, NUD identifies the specific facets in this orientation. Dimension statements limit NUD to values  $\leq 10$ .

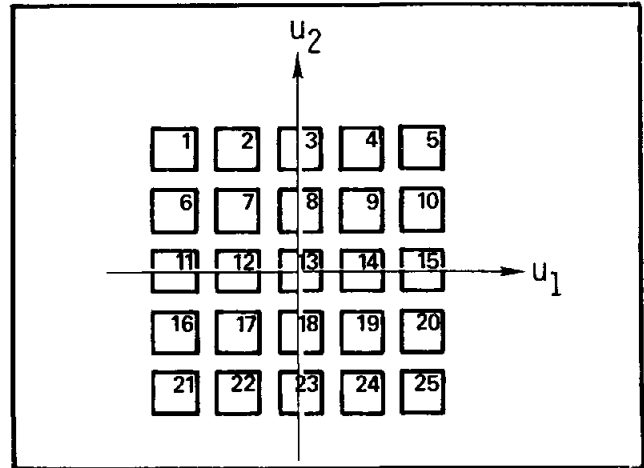


Figure 8. Plane Projection of Facet Array on One Heliostat

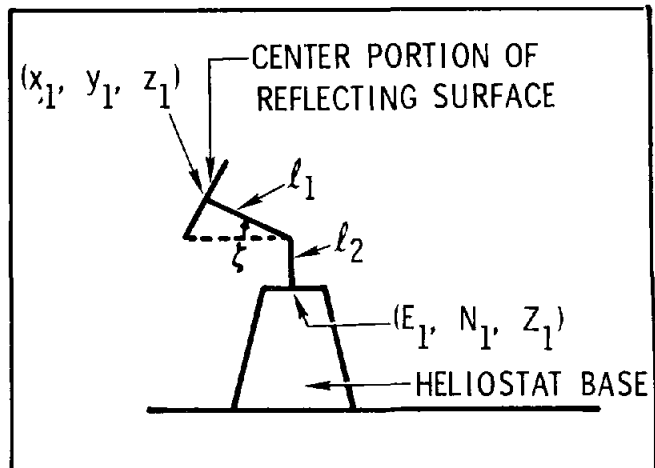
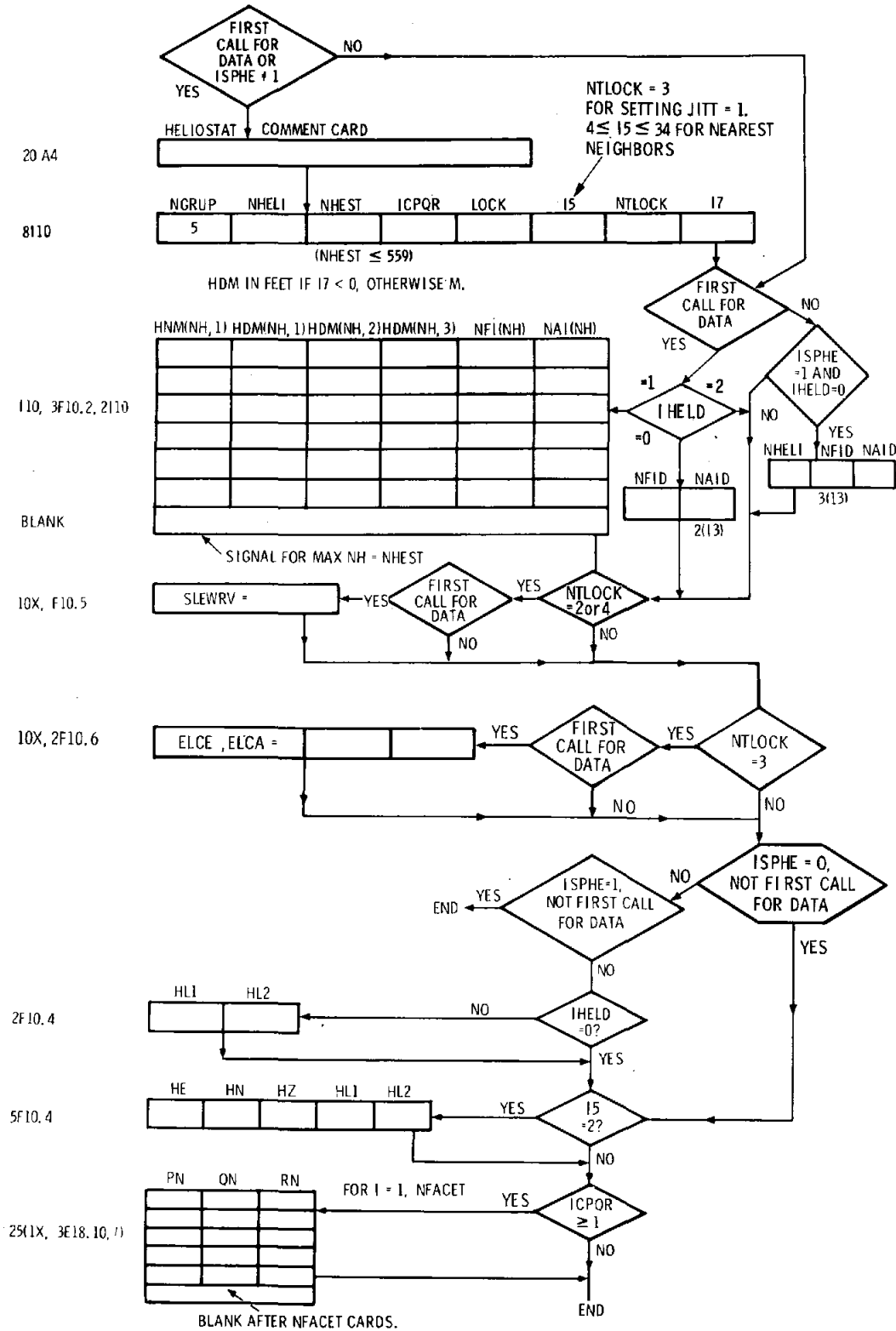


Figure 9. Sample Heliostat Mounting

# Group 5 Input Cards – Heliostat Parameters



## Options

- NGRUP = 5 Index verifies this is Group 5 data.
- NHELI = NHELI is an identification number for the first processed heliostat. The x, y, z (east, north, and vertical) coordinates of 534 CRTF heliostat bases are stored in data statements in Subroutine INDATA. The NHELI here specifies the appropriate set of these coordinates.
- NHEST = On the first call to INDATA, NHEST specifies the number of heliostats to be processed. Otherwise, the parameter is ignored.
- ICPQR = -2 ICPQR < 1 indicates that the normals to the individual facets on the heliostat are to be calculated. The normals are calculated from the focus point and the prealignment time of day (TFOC) and day of the year (DFOC).  
 ≥ 1 Value indicates that facet normals (PN(I), QN(I), RN(I), I = 1, NFACET in the heliostat coordinate system) are read in from cards. The Group 4 data must precede Group 5; so NFACET is known.  
 = -8 Value causes the heliostats to be focused on axis; i.e., at prealignment the sun is artificially placed in line with the focus point and heliostat center. Focusing does not occur with IOPT = 2. Focusing is automatic with IOPT = 5, independent of ICPQR.  
 = -3 Value causes the normals to the facet centers (PN(I), QN(I), RN(I), I = 1, NFACET) to be punched onto cards with format (1X, 3E 18.10). These cards may be used in a later computer run with ICPQR ≥ 1. The punching is done in Subroutine CPQR.
- LOCK = 0 LOCK = 0 causes the heliostat to follow the sun.  
 = 1 Value will lock the heliostat in the position of previous calculation. This option is useful for examining consequences of power failures.  
 = 2 Value will signal an emergency situation where the motors controlling the heliostat elevation angles are sluing to put the heliostats facedown for

storage. The elevation angle is reduced by subtracting the slue rate (SLEWRV in radians/hour) times the time transpired (since the earlier time of day processed) from the previous value of elevation angle. The slue rate in the CRTF is 19.6 rad/h.\* The azimuthal angle is not changed.

The azimuthal drive at the CRTF also has a slue speed of 19.6 rad/h. These are much faster than the maximum tracking motor speeds of 1.2 rad/h at the CRTF.

- = 4 Value indicates slue start of the heliostats. Each heliostat starts from a facedown position. The initial azimuthal angle is to the south (north) for heliostats to the north (south) of the tower. At later calculation times, the elevation angles are increased by the time interval times the slue rate. Once the elevation angle exceeds that resulting from regular tracking, regular tracking occurs. The sluing motors allow more rapid alignment on target. The option is included so that safety aspects of the approach can be studied.

15

- = 0, Value indicates that each heliostat is 1 tested for shadowing and blocking or against all other heliostats in the cell.  
 2 If 15 = 2, the x, y, and z coordinates (HE, HN, HZ) for the heliostat must be read in along with heliostat support dimensions HL1 and HL2. These data are obtained from NHELI and default values of HL1 (0.318 m) and HL2 (3.987 m) when ISPHE = 1; i.e., for the CRTF heliostats.

- = N Value N indicates that shadowing and blocking tests are for the N nearest neighbors to each heliostat rather than for all the heliostats in the field. Values  $4 \leq N \leq 34$  are valid. At early or late times of day, it is possible for a heliostat to be shadowed by several heliostats. In such cases N near 20 may give more accurate results than

\*The slue rate is expected to vary slightly with heliostat and with loading alterations.



testing all the heliostats in the field. The shadowing diagram will indicate such a situation when it occurs.

NTLOCK = 0 For NTLOCK = 0, the value of LOCK is controlled only by heliostat positioning data (Group 5). In this case only LOCK = 0 makes sense.

= 1,2 LOCK is set to 0 initially for each or heliostat and reset to NTLOCK after 4 the first time of day is processed.

= 3 Jitter is included in the heliostat aiming. A parameter JITT is set to 1 (from default value 0). The encoder least counts ELCE and ELCA (in radians) for elevation and azimuthal angles are required. The NTLOCK is reset to zero. It is not expected that jitter would ever be required for the emergency situations NTLOCK = 1 or 2. Subroutine JITTER is discussed in Appendix A of Part III in the user's guide

I7 = Index is used only when IHELD = 1. For I7 < 0 the HDM (NH,I) variables are input in feet. I7 ≥ 0 indicates values are in metres.

After the first call to INDATA and in the special case of ISPHE = 1 (Group 1), subsequent calls to INDATA only read NHELI, NFID, and NAID with HE, HN, and HZ determined from the data statements (or read from Tape 3 when IHELD = 2 in the Group 1 data). No other parameters may be changed in this special case. NFID specifies that the prealignment point for heliostat NHELI is XFOC(NFID), YFOC(NFID), and ZFOC(NFID). NAID specifies that the aim point for heliostat NHELI is XPOT(NAID), YPOT(NAID) and ZPOT(NAID). When NFID or NAID is 0 (or blank), its value is reset to 1.

If IHELD = 1, the Group 5 data must include identifying numbers (HNM(NH,1)) for each heliostat along with the tower coordinates ( $E_1, N_1, Z_1$  in Figure 10 - HDM (NH,I), I = 1,3) of each heliostat. This allows convenient insertion of a new heliostat field layout. The number of heliostats is limited to ≤ 559 at present.\* In this case HL1 and HL2 are also required input ( $l_1$  and  $l_2$  in Figure 9). The NFI(NH) and NAI(NH) specify the index for the appropriate prealignment point and aim point for heliostat NH. NFI and NAI input as blank or zero are reset to 1. The

heliostat identification number (HNM) must be an integer > 0.

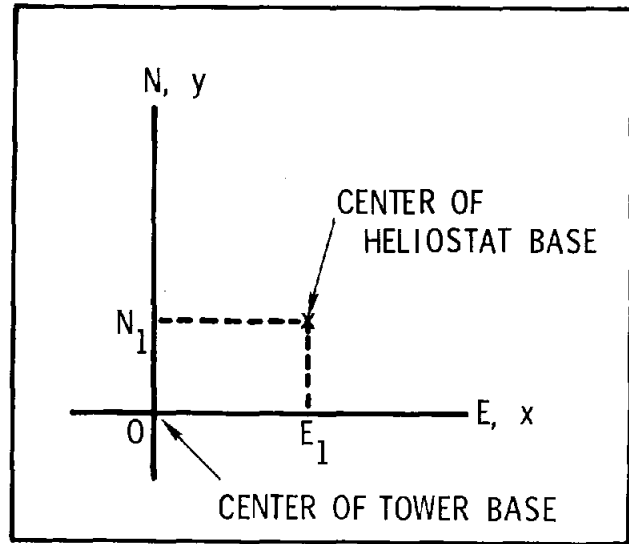
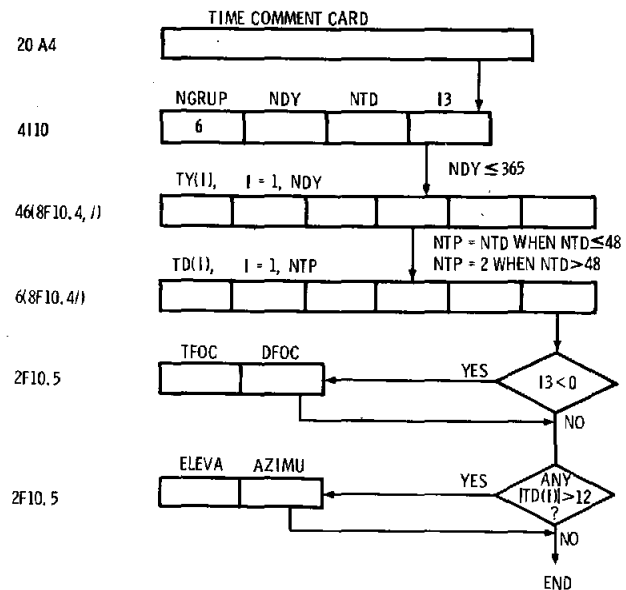


Figure 10. Heliostat Deployment in Tower Coordinate System

### Group 6 Input Cards – Time Parameters



### Options

- NGRUP = 6 Value verifies that this is Group 6 data.
- NDY = NDY is the number of days of the year to be processed.  $NDY \leq 365$ .
- NTD = NTD is the number of times of the day to be processed for each day of the year.
- I3 < 0 The time at which the facets are prealigned on the heliostat (time of day

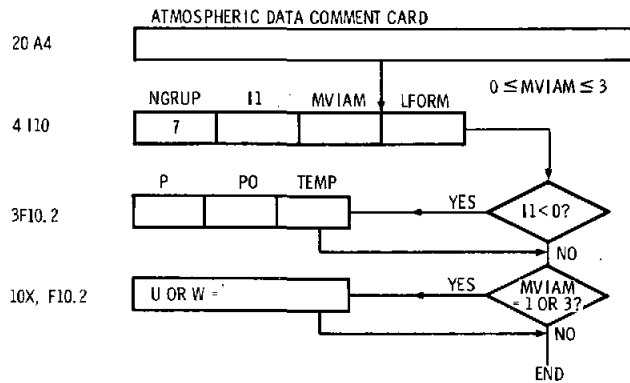
\*When IHELD = 2, more heliostats may be treated. There is a limit of 559 heliostats per cell.

(TFOC) and day of year (DFOC)) must be read in. Default values are 0.0 (noon) on Day 80 (March 21).

- TY(I) = TY gives the actual days to be processed.
- TD(I) = TD gives the actual times of the day to be processed. Here, time is measured in hours from local solar noon. Negative values indicate hours before local noon. The formats are such that if NDY or NTD is a multiple of 8, a blank card must follow the last TY or TD card. A TD (I) with absolute value >12 indicates the elevation and azimuthal (measured from east, positive toward north) angles of the sun are to be read (in degrees) from data cards rather than calculated for use at that time.

When NTD >48, only the extreme times, TD(1) and TD(2), are furnished. The NTD times of day occur in equal steps between the extremes. The initial time is repeated once for plotting convenience.

### Group 7 Input Cards – Atmospheric Parameters



### Options

- NGRUP = 7 Index verifies that this is Group 7 data.
- I1 = 1 I1 < 0 indicates that the variables P, PO, and TEMP are required. These are the atmospheric pressure in millibars, the standard sea level pressure in millibars, and the atmospheric temperature in degrees Celsius at the tower.
- MVIAM = 0 Index indicates that the model for variation of solar insolation with atmospheric mass is that developed by

Kondratyev. The models are explained in References 1 and 5.

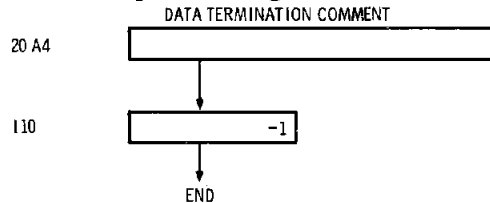
- = 1 The Allen model is used. The precipitable water overhead (W) is an input parameter.
- = 2 The Moon model is used. It is appropriate for W = 20 mm, ozone = 2.8 mm, and 300 aerosol particles/cm<sup>3</sup>.
- = 3 The Gates model is used. It is appropriate for W = 10 mm, ozone = 3.5 mm, and 200 aerosol particles/cm<sup>3</sup>. Here U is an input parameter <0.3.

The default value of MVIAM is 2. All the models are for clear days. When further atmospheric options are added and analytic representations of a series of sunshapes are available as some function of atmospheric conditions, Group 7 of the input cards is expected to grow in importance.

- LFORM = 0 Index indicates that the loss formula caused by propagation from mirrors to target is modeled in Subroutine PROP as developed in Section 6.3 of Reference 1.
- = 1 Propagation loss is reasonable for altitude 0.61 km\* above sea level (Barstow, CA) on a clear day.
  - = 2 Propagation loss is reasonable for altitude 0.61 km\* above sea level (Barstow, CA) on a hazy day at sea level.
  - = 3 Propagation loss is reasonable for altitude 1.52 km above sea level (Albuquerque, NM) on a clear day.
  - = 4 Propagation loss is reasonable for altitude 1.52 km above sea level on a hazy day at sea level.

At the end of a set of data cards, the following cards signal HELIOS that the input is complete. The cards are required even to complete the first problem set in the special case ISPHE = 1 (in the Group 1 data). They are not required after the list of heliostat numbers when ISPHE = 1 and IHELD = 1.

### Problem Input End Signal



\*Formulae for LFORM >0 are given by C. N. Vittitoe and F. Biggs in Reference 6. Also, see PROP Routine discussion in Part III for the formulae and for discussion of the "hazy day at sea level."

## IV. Interactive Preparation of Input File

The Network Operating System (NOS) at SNLA allows a computer user to interact with scientific computers through individual computer terminals (with typewriter and/or cathode-ray tube (CRT) communication) conveniently located throughout the laboratories. Once a data file is created on the system, editing procedures are available that are convenient for making small changes in the data. Methods are also available on NOS for directly submitting the job to larger computers for batch processing. Because such systems are becoming widespread, and since preparation of a data deck for HELIOS may require >100 computer cards, some users may desire an interactive system to generate data files. The DGENH2 (Data GENERation for HELIOS, version 2)

fulfills this need at the SNLA NOS system under user number CNVITTI or on public TFILE tape 11892.

The file DGENH2 is easily removed from the TFILE tape. The NOS command,

```
TFILE,R,011892,DGENH2,
```

takes the file from the public tape and stores it in the user's disk area as an indirect-access permanent file. Interaction with DGENH2 then creates a Tape 5 of input data for the HELIOS Code. Examples of the results of DGENH2 are presented in Part II, where sample problems are discussed. Below we illustrate use of DGENH2. On NOS the user responds to questions asked in capital letters. Lower case letters indicate the user's contribution. At the end of the example, the Tape 5 file is saved for use with HELIOS. The file can be punched for card-deck input or can be directly processed on the batch system by using NOS commands.

```
g,dgenh2
/ftn,i=dgenh2
S
      4.068 CP SECONDS COMPILATION TIME
/!go
WHICH DATA GROUP DO YOU WANT TO CHANGE?
8 TERMINATES DATA FOR A PROBLEM
OR FOR THE FIRST HELIOSTAT DATA SET
GT.8 TERMINATES THE DATA FILE
? 1
INPUT COMMENT CARD FOR NGRUP.
? king test problem for off-axis heliostat
GROUP 1 CHANGES,INSERT FOLLOWING VARIABLES
IPRINT,IPL0T1,ISHAD,IACCU,ISPHE,IHELD,IPROP
? 2,40,0,1,0,1,1
WHICH DATA GROUP DO YOU WANT TO CHANGE?
8 TERMINATES DATA FOR A PROBLEM
OR FOR THE FIRST HELIOSTAT DATA SET
GT.8 TERMINATES THE DATA FILE
? 2
INPUT COMMENT CARD FOR NGRUP.
? sun data for king test problem
GROUP 2 INPUT-SUN VARIABLES
INPUT INSOL
? 2
INSOL=2, WHAT IS INSOLATION (U/CM**2)?
? 0.0877
SUNSHAPE OPTION,JSUN = ?
? 7
DO YOU WANT TO USE DEFAULT SUNSHAPE OF A NARROW
EXPERIMENTAL DISTRIBUTION ? YES OR NO ?
? no
SUNSHAPE IN TABLE FORM, NTABL=?
? 19
INPUT THE NTABL VALUES OF TANGENT AND INTENSITY.
? 0.,18870
? .001,18710
? .002,18020
? .0025,17400
? .003,16540
? .0035,15290
? .00375,14400
? .004,12890
```

? .00425,9861  
 ? .0045,4755  
 ? .00475,1940  
 ? .005,226.5  
 ? .00525,65.27  
 ? .0055,27.64  
 ? .00575,21.63  
 ? .006,17.06  
 ? .0065,12.58  
 ? .007,10.33  
 ? .008,8.013  
 CONVOLUTION INDEX  
 ICON = 1 IMPLIES NUMERICAL  
 ICON= 2 IMPLIES ANALYTICAL- BOTH DISTRIBUTIONS GAUSSIAN  
 WITH RMS WIDTH OF EACH OBTAINED FROM DISTRIBUTION  
 ICON= 3 OR 0 GIVES CONVOLUTION ONLY WHEN SUN AND ERROR ARE  
 GAUSSIAN  
 ICON = ?  
 ? 5  
 INDEX I6 = ? (NEW SUNSHAPE PARAMETERS)  
 LT 0 INDICATES READ IN NEW PARAMETERS  
 FOR BET, FEPSUN, BLIM,ALO,AHI  
 ? 1  
 INPUT FOR INDIVIDUAL CONTRIBUTIONS TO UNCERTAINTY.  
 NUMBER OF SLOPE ERRORS IN HELIOSTAT SYSTEM NER=  
 ? 1  
 ARE TRACKING ERRORS NEGLECTED, YES ON NO  
 ? yes  
 NO.DIMENSIONS IN EFFECTIVE SUNSHAPE,1 OR 2  
 ? 2  
 IANLYT PARAMETER=  
 ? 0  
 ENTER NER SEPARATE CONTRIBUTIONS TO SLOPE ERROR  
 ERROR 1 ANGLE(DEG),SIGX,SIGY =  
 ? 0.,.00098,.00098  
 WHICH DATA GROUP DO YOU WANT TO CHANGE?  
 8 TERMINATES DATA FOR A PROBLEM  
 OR FOR THE FIRST HELIOSTAT DATA SET  
 GT.8 TERMINATES THE DATA FILE  
 ? 3  
 INPUT COMMENT CARD FOR NGRUP.  
 ? beam characterization system target data  
 HOW MANY TARGET POINTS: (NTART=1 TO 121)  
 ? 121  
 INDIVIDUAL FACET PRINT OUT FOR 3 TARGET POINTS  
 STARTING AT POINT NTARST WITH INTERVAL INUTR  
 READ NTARST,INUTR  
 ? 59,2  
 ITAR GT 0 ALLOWS TARGET CENTER TO BE READ IN  
 OTHERWISE AIM POINT OF FIRST HELIOSTAT IS TAKEN AS CENTER  
 ITAR =?  
 ? 1  
 IGEO =?  
 ? 0  
 IVMD=1 NORTH  
 2 NORTHEAST  
 3 EAST  
 4 SOUTHEAST  
 5 SOUTH  
 6 SOUTHWEST  
 7 WEST  
 8 NORTHWEST  
 9 DOWN  
 10 UP

IUMD=?  
 ? 1  
 IS PROPER TARGET ORIENTATION NEEDED? YES OR NO ?  
 ? yes  
 HOW MANY PREALIGNMENT POINTS DESIRED? (NFOC= 1 TO 20)  
 ? 1  
 SET PREALIGNMENT POINTS XFOC(I),YFOC(I),ZFOC(I)  
 COORDINATES OF POINT 1  
 ? 0.05,9.78,37.58  
 HOW MANY AIM POINTS ARE DESIRED ? (NPOIT= 1 TO 222)  
 ? 1  
 COORDINATES OF AIM POINT 1  
 ? 0.05,9.78,37.58  
 APERTURE PARAMETER IAPT =  
 ? 0  
 TOWER HEIGHT = ? (ZT USED FOR DEFAULT TARGET POSITION)  
 ? 37.5775  
 SITE LATITUDE =? PHIL FOR ALBUQUERQUE CRTF= 34.96  
 ? 34.96  
 TOWER HEIGHT, RADIUS AT TOP, RADIUS AT BOTTOM  
 FOR SHADOWING AND BLOCKING CALCULATION (IN METERS)  
 ZEF,EFWT,EFWB=?  
 ? 60.96, 7.5, 8.5  
 WHAT ARE THE HORIZONTAL AND ORTHOGONAL EXTENTS  
 OF THE TARGET SURFACE (XEXT,ZEXT)  
 ? 9.1436, 9.1436  
 TARGET SHAPE, ITARSH=0 RECTANGULAR  
 1 SPHERICAL  
 2 USER SUPPLIED  
 3 CYL-OUTWARD NORMAL  
 4 CYLINDRICAL -INWARD NORMAL  
 5 SQUARE,ORTHOGONAL TO CENTER RAY FROM FIRST HELIOSTAT  
 6 FLAT AND CIRCULAR  
 7 FLAT AND RECTANGULAR WITH RECONCENTRATORS  
 8-17 FLAT AND RECTANGULAR WITH DIVISION INTO SUBTARGETS  
  
 ITARSH = ?  
 ? 9  
 COORDINATES OF TARGET-MESH ORIGIN,UTAR(1,I=1,3) = ?  
 ? 0.05, 9.78, 37.58  
 SECOND POINT IN TARGET PLANE IS UTAR(2,I=1,3)=?  
 ? 4.57, 9.78, 37.58  
 THIRD POINT IN TARGET PLANE IS UTAR(3,I=1,3) = ?  
 ? 0.05, 10.26, 42.13  
 NUMBER OF TARGET POINTS ALONG HORIZONTAL AND  
 ORTHOGONAL DIRECTION  
 IXPTS,IYPTS=?  
 ? 11,11  
 WHICH DATA GROUP DO YOU WANT TO CHANGE?  
 8 TERMINATES DATA FOR A PROBLEM  
 OR FOR THE FIRST HELIOSTAT DATA SET  
 GT.8 TERMINATES THE DATA FILE  
 ? 4  
 INPUT COMMENT CARD FOR NGRUP.  
 ? facet data for barstow prototype, martin marietta design  
  
 NUMBER OF FACETS/HELIOSTAT = ? (UP TO 25)  
 ? 12  
 FACET SHAPE KORD=?  
 SQUARE 1,CIRCLE 2  
 RECTANGULAR 3, CIRCULAR WITH HOLE 4  
 EQUILATERAL TRIANGLES 5

KORD =  
 ? 3  
 FACET SUBDIVISION PARAMETER, NSUBF = ?  
 ? 0  
 FACET SURFACE SHAPE PARAMETER IOPT  
 1 PARABOLIC  
 2 FLAT  
 3 DISK TENSION  
 4 RING TENSION  
 5 SUPER SMART  
 6 SPHERICAL  
 7 USER ROUTINE  
  
 IOPT = ?  
 ? 7  
 LOADING PARAMETER NGL =  
 ? 0  
 WANT TO READ IN FACET LENGTH OR RADIUS ? YES OR NO?  
 ? no  
 WANT TO READ IN FACET REFLECTIVITY ? YES OR NO?  
 ? yes  
 REFLEC = ?  
 ? 0.89  
 RECTANGULAR SHAPE PARAMETERS ELENX,ELENY,NX,NY=  
 ? 3.0480, 1.0920, 13, 7  
 HELIOSTAT COORDINATES OF FACET CENTERS  
 U1,U2,U3 FOR FACET 1=?  
 ? -1.833, 2.857, 0.  
 U1,U2,U3 FOR FACET 2=?  
 ? +1.833, 2.857, 0.  
 U1,U2,U3 FOR FACET 3=?  
 ? -1.833, 1.714, 0.  
 U1,U2,U3 FOR FACET 4=?  
 ? +1.833, 1.714, 0.  
 U1,U2,U3 FOR FACET 5=?  
 ? -1.899, 0.571, 0.  
 U1,U2,U3 FOR FACET 6=?  
 ? +1.899, 0.571, 0.  
 U1,U2,U3 FOR FACET 7=?  
 ? -1.899, -0.571, 0.  
 U1,U2,U3 FOR FACET 8=?  
 ? +1.899, -0.571, 0.  
 U1,U2,U3 FOR FACET 9=?  
 ? -1.833, -1.714, 0.  
 U1,U2,U3 FOR FACET 10=?  
 ? +1.833, -1.714, 0.  
 U1,U2,U3 FOR FACET 11=?  
 ? -1.833, -2.857, 0.  
 U1,U2,U3 FOR FACET 12=?  
 ? +1.833, -2.857, 0.  
 INDICES FOR CORNER FACETS- CLOCKWISE,FACING HELIOSTAT  
 NC1,NC2,NC3,NC4 = ?  
 ? 1, 2, 12, 11  
 WHICH DATA GROUP DO YOU WANT TO CHANGE?  
 8 TERMINATES DATA FOR A PROBLEM  
 OR FOR THE FIRST HELIOSTAT DATA SET  
 GT.8 TERMINATES THE DATA FILE  
 ? 5

INPUT COMMENT CARD FOR NGRUP.  
 ? heliostat data for king off-axis test  
 DO YOU WANT HELIOSTAT COORDINATES IN FEET? YES OR NO  
 ? no  
 LOCK PARAMETERS LOCK,NTLOCK =?  
 ? 0,0  
 PREALIGNMENT OPTION, ICPQR=-2 NORMALS CALCULATED  
 -3 NORMALS CALCULATED AND PUNCHED ONTO CARDS  
 -8 NORMALS CALCULATED FROM ON-AXIS ALIGNMENT  
 GE 1 NORMALS READ IN  
 ICPQR =?  
 ? -2  
 HELIOSTAT IDENT,COORDINATES,PREALIGN,AND AIM INDICES  
 HNM,HDM1,2,3,NFI,NAI=?,HNM LE 0 INDICATES END  
 HELIOSTAT 1 SET  
 ? 1, 6.08, 320.03, 0.57, 1, 1  
 HELIOSTAT 2 SET  
 ? -1  
 ? 0,0,0,0,0  
 HELIOSTAT PARAMETERS HL1,HL2 = ?  
 ? 0.114, 3.784  
 WHICH DATA GROUP DO YOU WANT TO CHANGE?  
 8 TERMINATES DATA FOR A PROBLEM  
 OR FOR THE FIRST HELIOSTAT DATA SET  
 GT.8 TERMINATES THE DATA FILE  
 ? 6  
 INPUT COMMENT CARD FOR NGRUP.  
 ? time data for king off-axis test  
 NDY,NTD= ?  
 ? 1, 1  
 TFOC,DFOC INPUT IF I3.LT.0.  
 I3=?  
 ? -1  
 TFOC,DFOC= ?  
 ? -0.3370, 171.  
 DAY 1 =?  
 ? 255.  
 TIME 1= ?  
 ? 3.199  
 WHICH DATA GROUP DO YOU WANT TO CHANGE?  
 8 TERMINATES DATA FOR A PROBLEM  
 OR FOR THE FIRST HELIOSTAT DATA SET  
 GT.8 TERMINATES THE DATA FILE  
 ? 7  
 INPUT COMMENT CARD FOR NGRUP.  
 ? atmospheric data  
 WANT TO CHANGE PRESSURE OR TEMPERATURE ? YES OR NO ?  
 ? no  
 PICK ATMOSPHERIC MODEL, MUIAM= ? (0 TO 3)  
 0 KONDRATYEV  
 1 ALLEN  
 2 MOON  
 3 GATES  
 ? 2  
 PROPAGATION LOSS PARAMETER,LFORM =  
 ? 3  
 WHICH DATA GROUP DO YOU WANT TO CHANGE?  
 8 TERMINATES DATA FOR A PROBLEM  
 OR FOR THE FIRST HELIOSTAT DATA SET  
 GT.8 TERMINATES THE DATA FILE  
 ? 9

.321 CP SECONDS EXECUTION TIME.

xedit,tape5  
 XEDIT VER.SLA.8.1C REVISED 80/11/09. 19.35.54.  
 TAPES IS EDIT FILE

>? p30  
 KING TEST PROBLEM FOR OFF-AXIS HELIOSTAT  
 1 2 40 0 1 0 1 1  
 SUN DATA FOR KING TEST PROBLEM  
 2 2 7 1 1 1 1 5  
 SUN DATA = .877E-01 WATTS/CM\*\*2

19  
 0.00000 188.70000  
 .00100 187.10000  
 .00200 180.20000  
 .00250 174.00000  
 .00300 165.40000  
 .00350 152.90000  
 .00375 144.00000  
 .00400 128.90000  
 .00425 98.61000  
 .00450 47.55000  
 .00475 19.40000  
 .00500 2.26500  
 .00525 .65270  
 .00550 .27640  
 .00575 .21630  
 .00600 .17060  
 .00650 .12580  
 .00700 .10330  
 .00800 .08013

1 0 2 0 0 1.00000  
 0.00 .980E-03 .980E-03  
 BEAM CHARACTERIZATION SYSTEM TARGET DATA  
 3 121 59 2 1 0 1 2  
 1 1 0  
 37.5775 34.9600 9.1436 9.1436 .0500 9.7800 37.5800 60.9600  
 7.5000 8.5000  
 .05 9.78 37.58 4.57 9.78 37.58 .05 10.26 42.13  
 .05 9.78 37.58

11 11 9 0  
 FACET DATA FOR BARSTOW PROTOTYPE, MARTIN MARIETTA DESIGN  
 4 12 3 0 7 1 -1 0  
 3.0480 1.0920 13 7  
 REFLEC = .8900  
 -1.8330 2.8570 0.0000  
 1.8330 2.8570 0.0000  
 -1.8330 1.7140 0.0000  
 1.8330 1.7140 0.0000  
 -1.8990 .5710 0.0000  
 1.8990 .5710 0.0000  
 -1.8990 -.5710 0.0000  
 1.8990 -.5710 0.0000  
 -1.8330 -1.7140 0.0000  
 1.8330 -1.7140 0.0000  
 -1.8330 -2.8570 0.0000  
 1.8330 -2.8570 0.0000

1 2 12 11  
 HELIOSTAT DATA FOR KING OFF-AXIS TEST  
 5 1 1 -2 0 0 0 1  
 1 6.08 320.03 .57 1 1  
 -1 0.00 0.00 0.00 0 0  
 .1140 3.7840

TIME DATA FOR KING OFF-AXIS TEST  
 6 1 1 -1  
 255.0000  
 3.1990  
 -.33700 171.00000



```

ATMOSPHERIC DATA
  7
DATA TERMINATION FOR HELIOS CALCULATION 1 2 3
  -1 -1
END OF FILE

```

For punching data cards over the NOS system:

```
route(tape5,dc=ph)
```

## V. CELL Code Preparation of Tape 3 for IHELD = 2

The Helios Code is arranged as a series of DO loops: over day and time in the main overlay HELIOS and over a series of other parameters in the prealignment overlay (A), in the alignment, shadowing, and blocking overlay (B), and in the flux-density calculation overlay (C). The series of other parameters now includes loops over cells, heliostats within cells, facets on each heliostat, reconcentrator surfaces, target points on target and on reconcentrators, and over the elements of each area on a facet. Some heliostat fields are expected to contain thousands of heliostats. To make the Code more efficient in such cases, the field is divided into cells. IHELD = 2 specifies that the cell option is to be used. Otherwise only one cell is treated. Careful ordering of information on Tape 3 increases efficiency for processing multiple heliostat data through these loops.

Because of the DO-loop ordering, the heliostats are listed by cell on Tape 3. Within each cell the heliostats are ordered according to their closeness to the cell-centroid defined later. Heliostats within a cell have small angular separations as viewed from a point near the receiver. Shadowing and blocking calculations for the first heliostat in the cell (that nearest the centroid) can then be used to approximate shadowing and blocking for all heliostats in the cell. The flux-density distribution from this first heliostat might also be used to approximate the distribution from each heliostat in the cell. Correction factors might be applied to adjust for differing distances from each heliostat or for slightly different angles of incidence. The distributions might be shifted spatially to adjust for varying aim point for heliostats within a cell. All these factors are not included in the present form of cell option in HELIOS.

The cell option in HELIOS now calculates shadowing and blocking for the first heliostat in a cell and uses the same value for all heliostats with a cell. The flux-density calculations are performed for each heliostat. In this option the 559-heliostat limit no longer

applies. Any number of heliostats may be treated; i.e., within limitations of computer time and tape length. However, the number of heliostats within one cell is required to be  $\leq 559$ . If extensive application of HELIOS to large fields is anticipated, approximations in terms of the first heliostat, correction factors, and distribution shifts should be implemented.

Figure 11 is a flow diagram showing the information on Tape 3. Recall that within each cell the heliostats are listed in order of increasing distance from the cell centroid. This ordering is done automatically within the cell code. Each rectangle in the diagram represents one unformatted record on the tape. The variables are defined where the cell geometry is explained.

### Cell Geometry

Bounds for the cell geometry are indicated in the tower coordinates of Figure 12. The azimuthal angles are in radians within  $-\pi < \phi \leq \pi$ . Radial bounds are designated by R1, R2. The limiting variables  $\phi_1, \phi_2, R1, R2$  are all measured in the x,y plane.

Preliminary to defining individual cells, we tabulate several relationships between angles. Figure 13 shows an arc S generated by a change  $\delta\phi$  in the azimuthal angle  $\phi$ . However, it is the angle  $\delta\beta$  that this arc generates from the viewpoint of the cell-structure aim-point that we wish to limit within a single cell.

For convenience here, and without any loss of generality, we scale the geometry so that the distance from the cell-structure aim-point to a point on the x-axis at angle  $\eta$  is unity as indicated by the unit vector  $\hat{a}$ . Rotation by  $\delta\phi$  about the z-axis would move the unit vector to position  $\hat{b}$  as shown. The unit vectors  $\hat{a}$  and  $\hat{b}$  are given by

$$\hat{a} = (\sin \eta, 0, -\cos \eta) \quad (1)$$

$$\hat{b} = (\sin \eta \cos(\delta\phi), \sin \eta \sin(\delta\phi), -\cos \eta) \quad (2)$$

where we are using the notation (x, y, z) for the components of a vector. From this we get

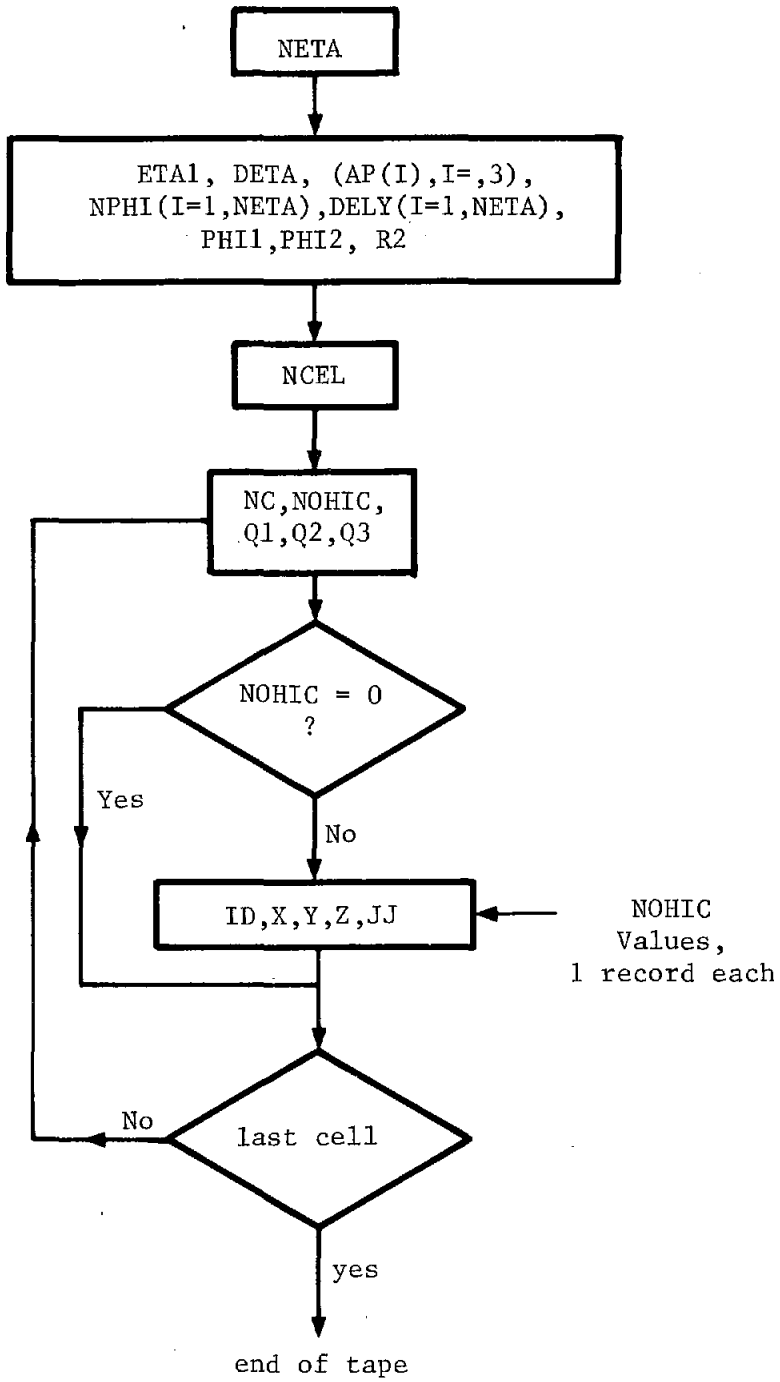


Figure 11. Data Organization for Tape 3

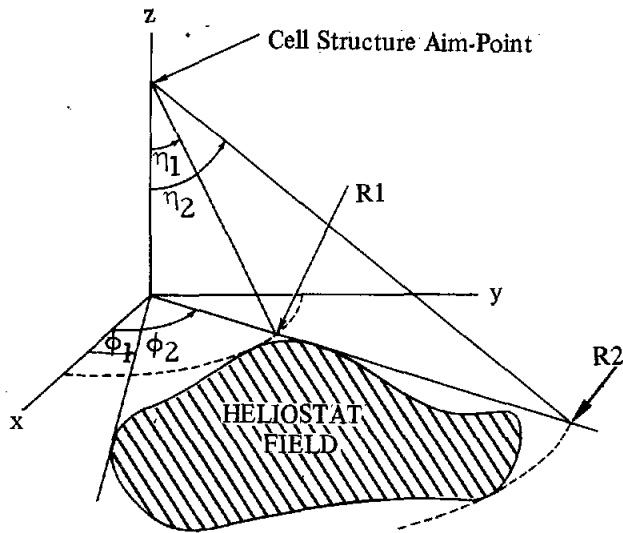


Figure 12. Cell Boundary Geometry

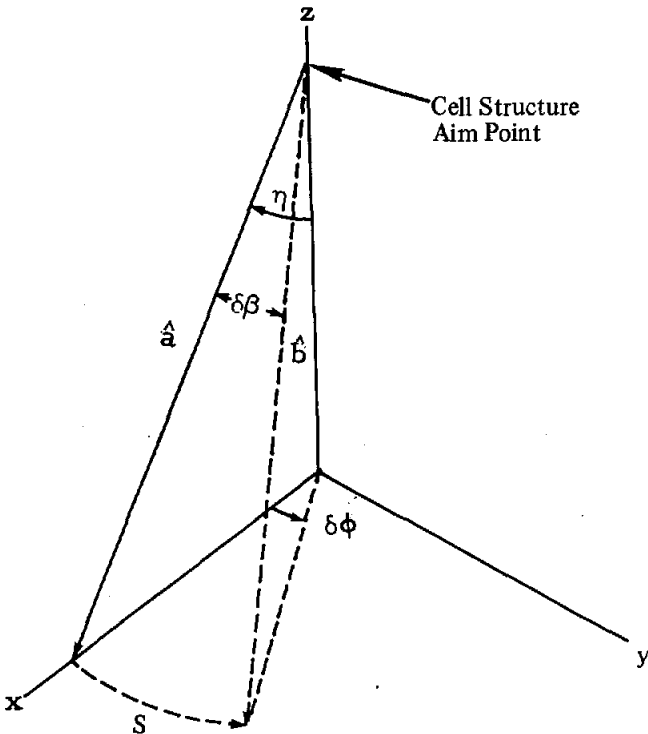


Figure 13. Cell Angular Interval Geometry

$$\cos(\delta\beta) = \hat{a} \cdot \hat{b} = \sin^2\eta \cos(\delta\phi) + \cos^2\eta \quad (3)$$

If  $\delta\beta$  and  $\delta\phi$  are small enough that we can ignore everything after the  $\theta^2/2$  term in the expansion

$$\cos \theta = 1 - \frac{\theta^2}{2} + \frac{\theta^4}{4!} - \dots, \quad (4)$$

then Eq (3) simplifies to

$$\delta\beta \approx \delta\phi \sin \eta. \quad (5)$$

Although we do not use this approximation in the cell code, it is useful for the reader to use in visualizing trends.

The bounding field is divided into cells so that the angular dimension  $\delta\eta$  of a cell and  $\delta\beta$  across the outer arc of a cell are approximately equal and do not exceed a specified value  $\delta\gamma$ .

If  $\eta$  changes by an amount  $\delta\gamma$  and  $\phi$  changes so that  $\delta\beta$  is also equal to  $\delta\gamma$ , the result of both of these changes  $\delta\omega$  as viewed from the cell-structure aim-point is obtained by using a result from right spherical triangles,

$$\cos(\delta\omega) = \cos^2\delta\gamma. \quad (6)$$

The geometry for these angles is shown in Figure 14. If both these angles are small compared to 1 rad, then

$$\delta\omega = \sqrt{2} \delta\gamma, \quad (6a)$$

which may be useful to estimate the Code input parameter  $\delta\gamma$ .

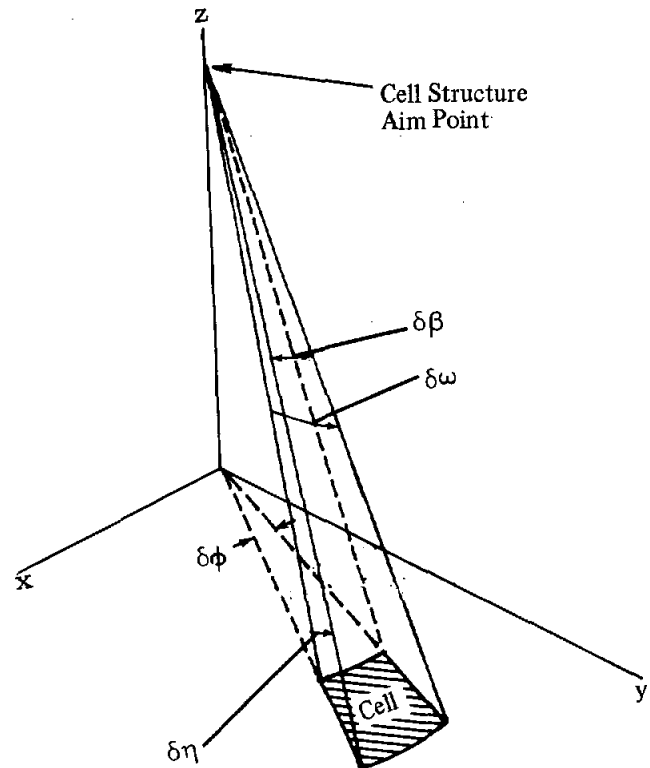


Figure 14. Angular Limits for a Cell

We first divide the bounding field into NETA radial zones

$$\text{NETA} = \text{INT} \frac{\eta_2 - \eta_1}{\delta\gamma} + 1, \quad (7)$$

where  $\eta_1$  and  $\eta_2$  are the angles shown in Figure 12 that correspond to the radial limits R1 and R2. The angular width of these radial zones as viewed from the initial aim-point is

$$\text{DETA} = (\eta_2 - \eta_1) / \text{NETA}. \quad (8)$$

Note that unless  $(\eta_2 - \eta_1)$  is a multiple of  $\delta\gamma$ , this will define the radial zones with  $\delta\eta < \delta\gamma$ .

From Eq (3), we get the change  $\delta\phi$  corresponding to a change  $\delta\beta = \delta\gamma$  of

$$\delta\phi(I) = \arccos \left\{ \frac{\cos(\delta\gamma) - \cos^2(\eta(I))}{\sin^2(\eta(I))} \right\}, \quad (9)$$

where

$$\eta(I) = \eta_1 + I * \text{DETA} \quad (10)$$

is the value of  $\eta$  corresponding to the outer arc of Zone I and  $\eta_1$  is the lower limit of  $\eta$  on the bounding field.

We now define the number of cells in radial Zone I by

$$\text{NPHI}(I) = \text{INT} \left[ \frac{\phi_2 - \phi_1}{\delta\phi(I)} \right] + 1. \quad (11)$$

The corresponding width of cells in Zone I is

$$\text{DELY}(I) = (\phi_2 - \phi_1) / \text{NPHI}(I). \quad (12)$$

When Eq (9) is used to estimate  $\delta\phi(I)$  and is used in Eq (11), it is evident that NPHI(I) will generally increase with increasing I.

The CELL Code determines the cell to which any heliostat is assigned without resorting to bisection search. Thus, the time required to partition the bounding field is merely proportional to the number of heliostats.

If correction factors were to be inserted so that the first heliostat in each cell could serve as the flux-density calculator for all, then the factors might be inserted most conveniently in Program C of HELIOS, after heliostat aiming is determined (in B) along with angles of incidence, and where spatial distributions of flux density might be shifted as the aim-point

varies for heliostats within a cell. An alternative is for correction factors to be calculated in B (one of the fastest portions of the HELIOS Code) and transferred to C by means of Tape 11. The shifting to account for aim-point variation must be done in C.

## CELL Code Input and Output

The CELL Code consists of about 200 source statements plus 75 comment statements. As seen in the code listing in Appendix B, cell variables are inserted directly in the Code. Those parameters set by the user are

- MRADZ - maximum number of radial zones
- MNTOT - maximum number of cells
- MNHIC - maximum number of heliostats per cell (559 for HELIOS)
- AP(I=1,3) - tower coordinates of cell-structure aim-point
- R1,R2 - inner and outer radii limits
- PHI1,PHI2 - azimuthal limits to heliostat field ( $\phi_1, \phi_2$ )
- DANG - maximum angular dimensions of a cell ( $\delta\gamma$  in radians)

The Code then calculates the bounds  $\text{ETA1}(\eta_1)$ ,  $\text{ETA2}(\eta_2)$ , and the parameters  $\text{NETA}$ ,  $\text{DETA}$ ,  $\text{NPHI}(I=1, \text{NETA})$ ,  $\text{DELY}(I=1, \text{NETA})$ . Other variables to be determined require the heliostat data.

Examination of the CELL Code listing along with its Subroutine CELNUM indicates how heliostat coordinates are translated into a specific cell number (NC). The heliostat data are read from Tape 1. In present form, the data contain x, y, z coordinates for each heliostat base. The initial record on Tape 1 gives the number of heliostats listed. The heliostats come in arbitrary order. CELNUM assigns the appropriate cell number (NC). The identification number (ID) is assigned sequentially starting with 1 for the first heliostat on Tape 1. Subsequent processing of the data yields the number of heliostats within each cell (NOHIC) and the coordinates for the cell centroid

$$Q_\alpha = \frac{1}{\text{NOHIC}} \sum_{i=1}^{\text{NOHIC}} d_i,$$

where  $\alpha = 1, 2, 3$  for  $d_i = x, y, z$  respectively. The summation is over heliostats within a given cell. NCEL contains the total number of cells within the heliostat field.

Code output is the Tape 3 data in the order described by the flow diagram noted earlier. Once the

tape is generated, that heliostat field need no longer be processed by CELL. Although for a large field the Code may require 1000 s of CDC 7600 time (700 s for 12000 heliostats), Tape 3 is then available for many HELIOS runs.

As an example of the variation in cell size around the field, Figure 15 gives the cell structure resulting from the CELL Code with input as listed in Appendix B. Figure 16 indicates heliostat assignments within the cells for a problem with different cell structure. The plotting codes are discussed together in Part IV of the user's guide.

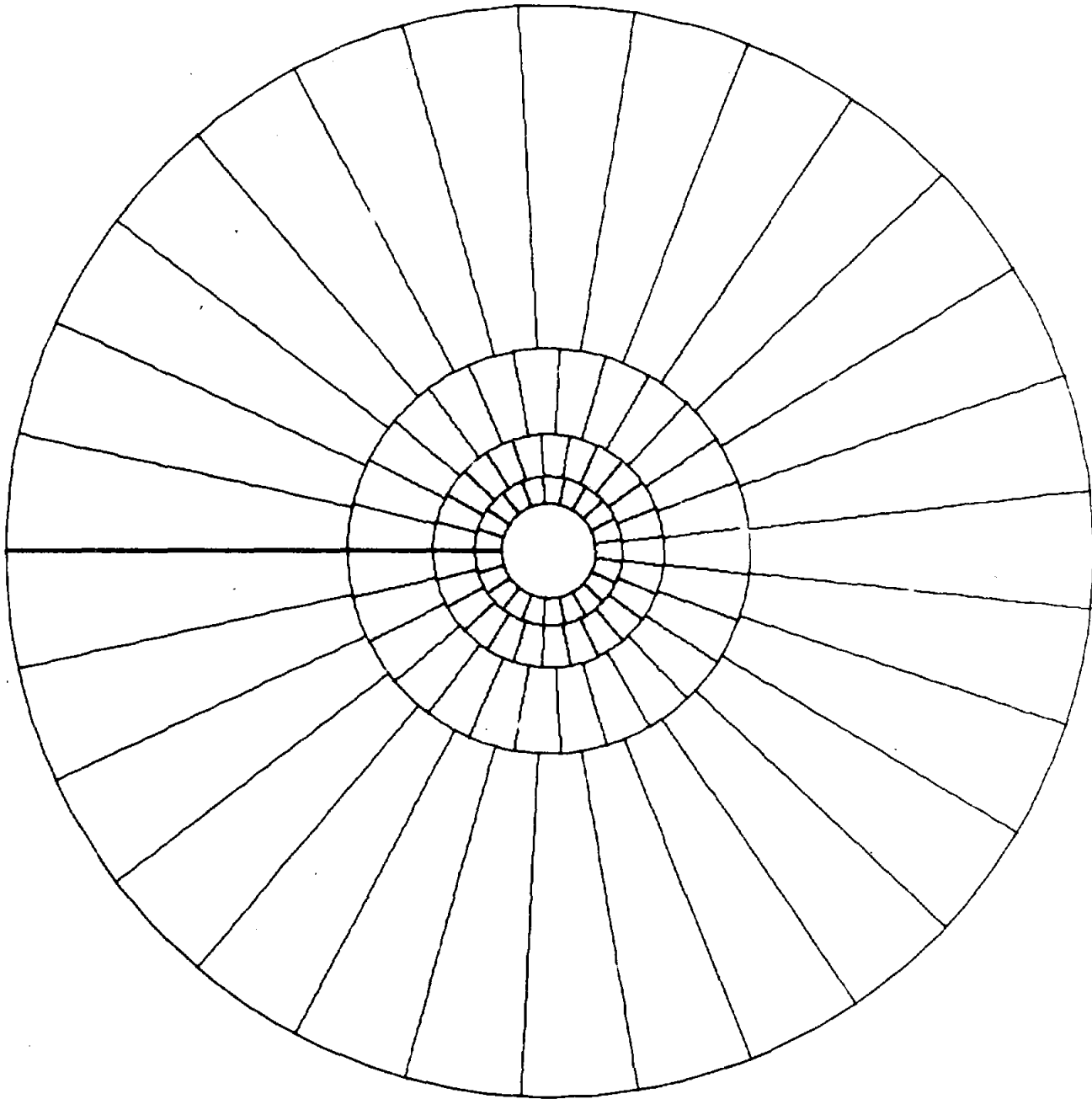


Figure 15. Cell Structure Resulting From CELL Input as in Appendix B

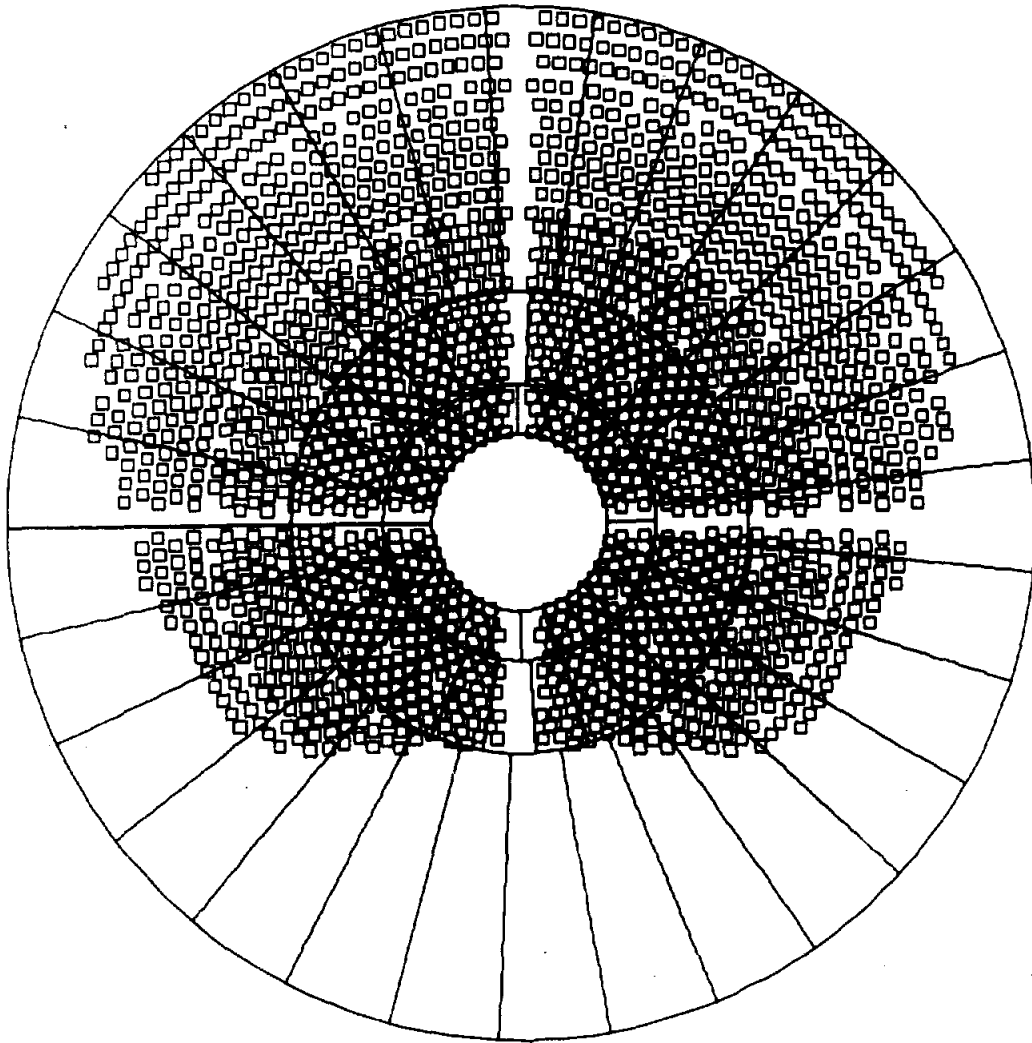


Figure 16. Cell Structure With an Example of Heliostat Assignments

## References

<sup>1</sup>F. Biggs and C.N. Vittitoe, *The Helios Model for the Optical Behavior of Reflecting Solar Concentrators*, SAND76-0347 (Albuquerque, NM: Sandia Laboratories, March 1979).

<sup>2</sup>A. Hunt, D. Grether, and M. Wahlig, "Circumsolar Radiation Data for Central Receiver Simulation," *Proceedings of the ERDA Solar Workshop on Methods for Optical Analysis of Central Receiver Systems*, University of Houston, Houston, TX, August 10-11, 1979 (also Lawrence Berkeley Laboratory Report Number LBL8371, August 1978).

<sup>3</sup>A. D. Watt, *Circumsolar Radiation*, SAND80-7009 (Albuquerque, NM: Sandia National Laboratories, April 1980), p 193.

<sup>4</sup>C. N. Vittitoe, F. Biggs, and P. L. Leary, *Comparison Between Results of the HELIOS and MIRVAL Computer Codes Applied to Central Receiver Solar-Energy Collection*, SAND79-8266 (Albuquerque, NM: Sandia National Laboratories, January 1980).

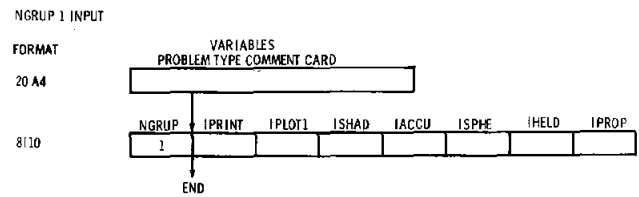
<sup>5</sup>L. L. Vanthull, "Methods for Estimating Total Flux in the Direct Solar Beam at Any Time," Vol 1 of *Proceedings of the Sharing the Sun Solar Technology in the Seventies Joint Conference of the International Solar Energy Society and the Solar Energy Society of Canada, Inc.*, ed K. W. Boer, August 15-20, 1976, Winnipeg, Canada, p 369.

<sup>6</sup>C. N. Vittitoe and F. Biggs, "Terrestrial Propagation," Vol 2.2 of *Proceedings of the 1978 Annual Meeting of the American Section of the International Solar Energy Society*, Denver, CO, August 28-31, 1978, pp 664-668.

# APPENDIX A

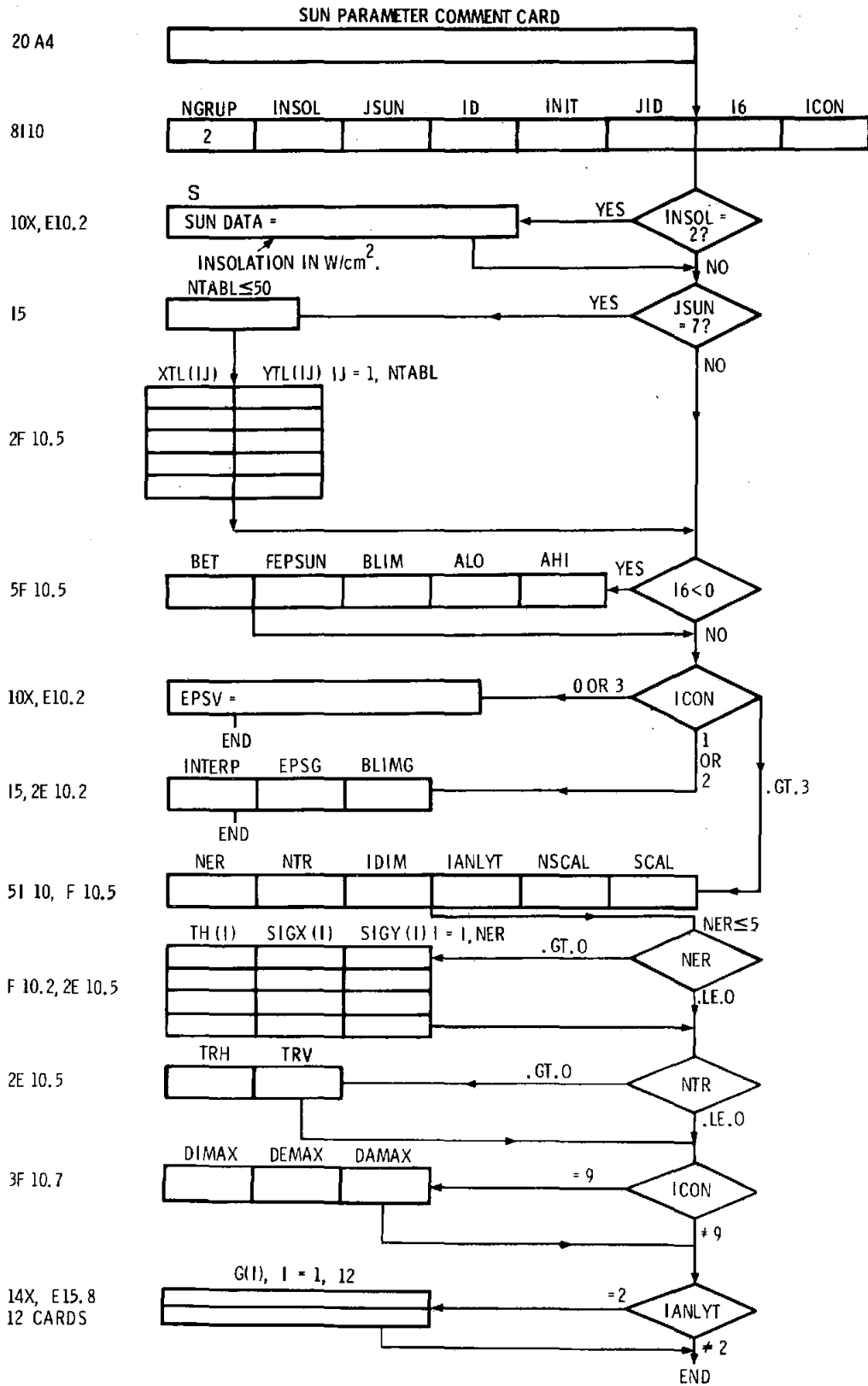
## Input Flow Charts

Input flow charts have been repeated here to facilitate gathering data for specific problems of interest to the user. Copies may be useful for recording problem parameters for later punching of cards or typing into computer storage.





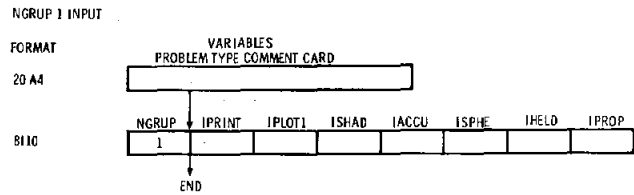
NGRUP 2 INPUT



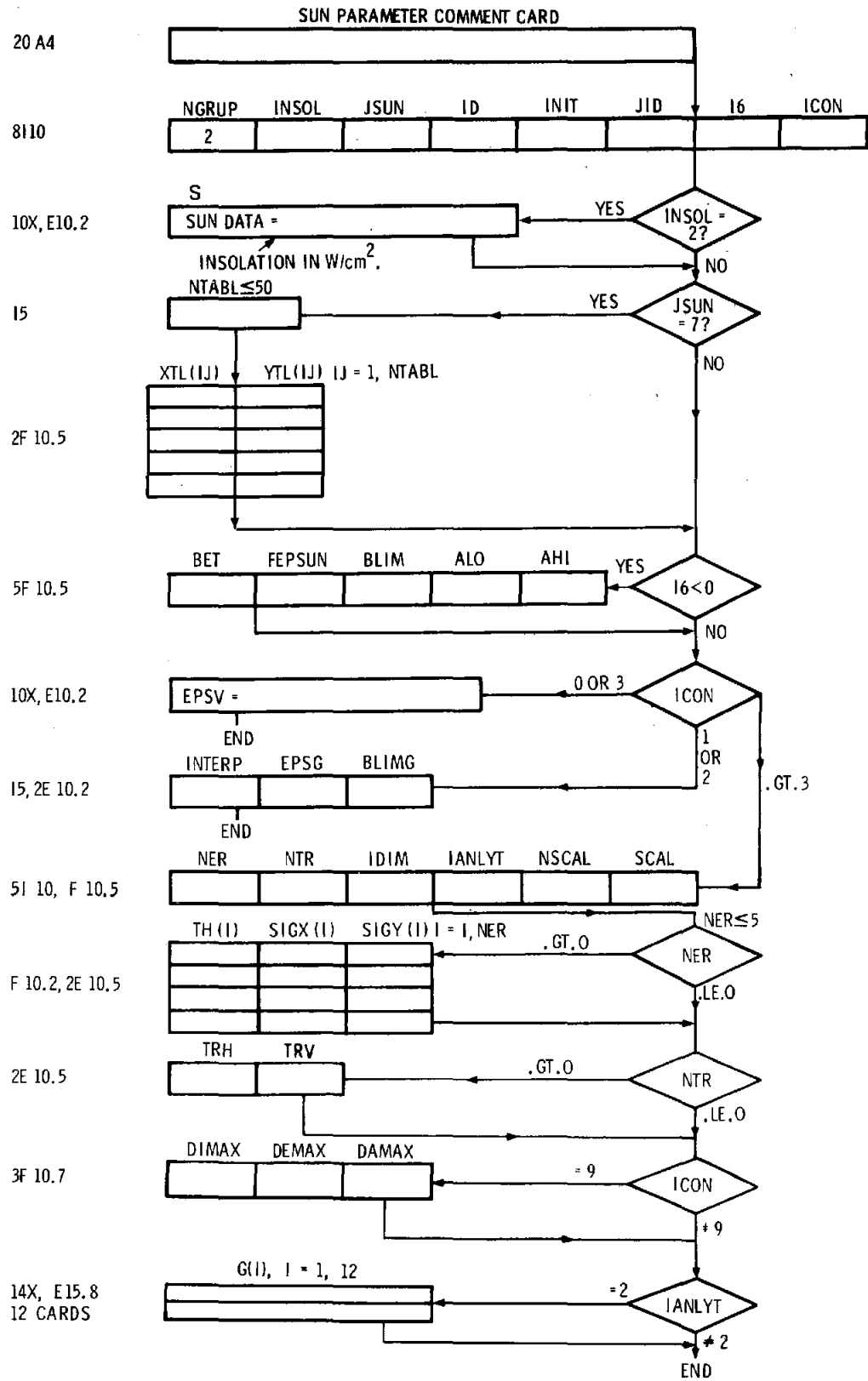
# APPENDIX A

## Input Flow Charts

Input flow charts have been repeated here to facilitate gathering data for specific problems of interest to the user. Copies may be useful for recording problem parameters for later punching of cards or typing into computer storage.



NGRUP 2 INPUT



NGRUP 3 INPUT

TOWER RECEIVER COMMENT CARD

NTART = 1 - NO POWER INTEGRATION  
 NTART ≠ 121 - POWER INTEGRATION  
 MUST BE CHANGED

20 A4

NGRUP	NTART	NTARST	INVTR	ITAR	IGEO	IVMD	17
-------	-------	--------	-------	------	------	------	----

8110

3							
---	--	--	--	--	--	--	--

3110

NFOC	NPOIT	IAPT	
------	-------	------	--

(NTART ≤ 121)

NFOC > 1

NPOIT > 1

YES

XFOC (I)	YFOC (I)	ZFOC (I), I=1, NFOC

YES I = 1, NPOIT

XPOT (I)	YPOT (I)	ZPOT (I)

3F10.5

3F10.5

AC (I, J), J = 1, 3


I = 1  
 I = 2  
 I = 3  
 I = 4

IAPT > 0

3F10.5

ZT	PHIL	XEXT	ZEXT	XPOIT	YPOIT	ZPOIT	ZEF
----	------	------	------	-------	-------	-------	-----

2(8F 10.4, /)

EFWT	EFWB
------	------

9F8.2

VTAR(1, 1)	(1, 2)	(1, 3)	(2, 1)	(2, 2)	(2, 3)	(3, 1)	(3, 2)	(3, 3)
------------	--------	--------	--------	--------	--------	--------	--------	--------

17 ≥ 0?

3F8.2

HEFOC	HNFOC	HZFOC
-------	-------	-------

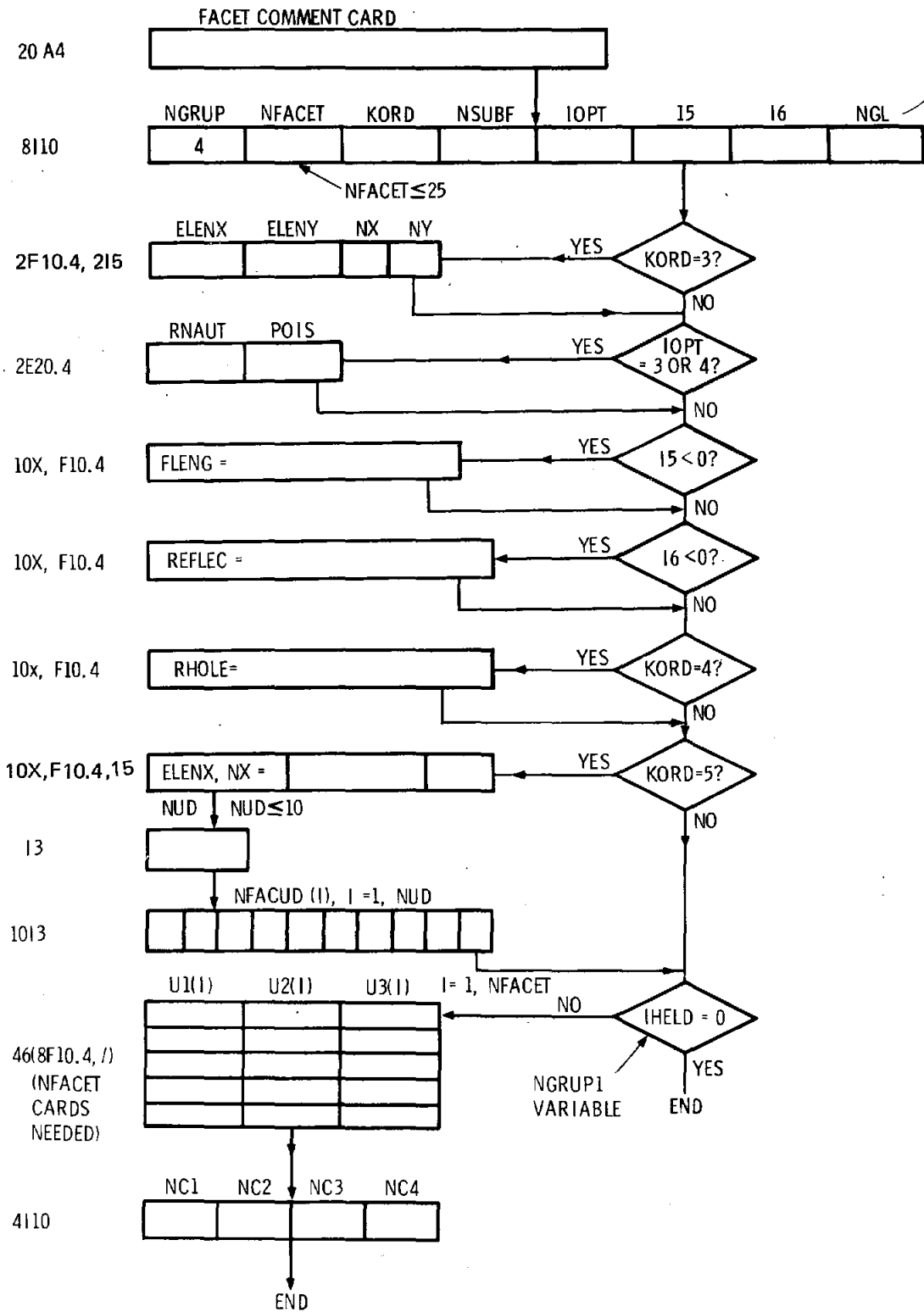
171 = 2?

4110

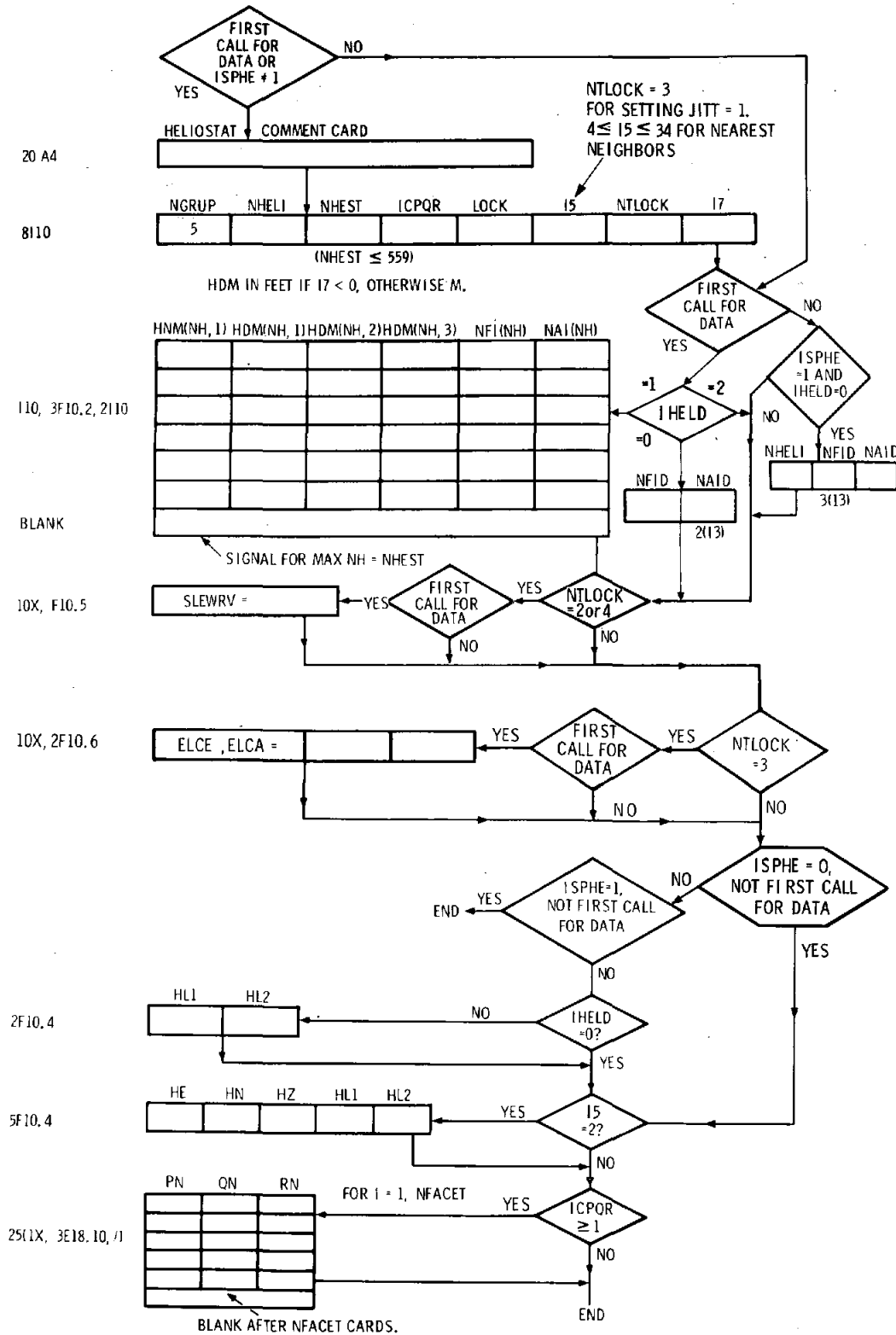
IXPTS	IYPTS	ITARSH	IRECP
-------	-------	--------	-------

END

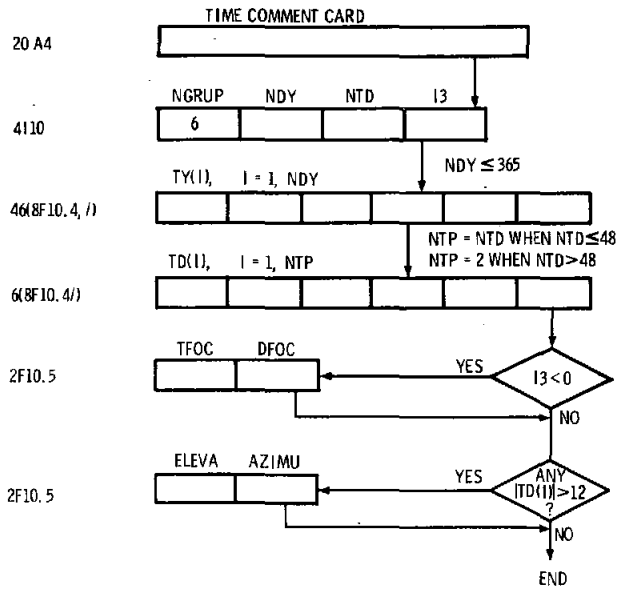
NGRUP 4 INPUT



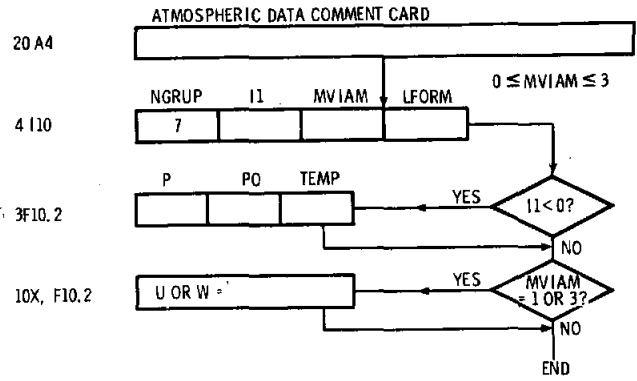
NGRUP 5 INPUT



NGRUP 6 INPUT



NGRUP 7 INPUT



## APPENDIX B

### CELL Code Listing

The CELL Code prepares a Tape 3 for proper acceptance by HELIOS when IHELD = 2. The code will require change because of variations in the form of heliostat coordinates (card or tape formats) and in

the cell structure desired. The Code uses the mathematical library routine SSORT that will order N variables Z(I) in order of increasing Z(I) while carrying along a second matrix (in this case the corresponding heliostat identification numbers) IDH(I).

```
PROGRAM CELL(TAPE1,TAPE2,TAPE3,OUTPUT=101B,TAPES=OUTPUT,
*TAPE4,INPUT=101B, TAPE66=INPUT, TAPE77=101B)
DIMENSION AP(3), ZIC(559), IDH(559)
COMMON /CCEL/ ETA1, ETA2, DELTA, NPHI(15), DELY(15)
COMMON /UK/ NTOT(130)
NOUT = 6
C
C ***** SET DIMENSION OF NPHI, DELY = MAXIMUM NUMBER OF
C RADIAL ZONES.
C NRADZ = 15
C
C ***** SET DIMENSION OF NTOT =MAXIMUM NUMBER OF CELLS
C NNTOT = 130
C
C ***** SET MAX NO.OF HELIOSTATS PER CELL; I.E.DIMENSION
C OF ZIC, IDH
C NPHIC = 559
C
C ***** SET PRINT OUT INDEX, IPRINT = 1 FOR INDIVIDUAL
C HELIOSTAT PRINT OUT.
C IPRINT = 1
C
C ***** SET COORDINATES OF AIM POINT FOR CELL DIVISION -AP
C
C AP(1) = 0.
C AP(2) = 0.
C AP(3) = 205.
C
C ***** SET INNER AND OUTER RADII LIMITS - R1, R2
C
C R1 = 130.
C R2 = 1500.
C
C ***** SET LOWER AND UPPER AZIMUTHAL ANGLE LIMITS
C TO HELIOSTAT FIELD - PHI1, PHI2 IN RADIANS
C PHI1 = -4.*ATAN(1.)
C PHI2 = 4.*ATAN(1.)
C
C ***** SET MAXIMUM ANGULAR DIMENSIONS OF A CELL -
C DANG, IN RADIANS
C DANG = .22
C
C WRITE (NOUT,99999) (AP(I),I=1,3), R1, R2, PHI1, PHI2, DANG
99999 FORMAT (1H1, /, 5X, 16HCELL DESCRIPTION, /, 10X, 11HAIM POINT =,
* 3F10.3, /, 10X, 10HR LIMITS =, 2F10.3, /, 10X, 14HAZIMUTHAL ANGL,
* 10HE LIMITS =2F10.3, 8H RADIANS, /, 10X, 20HMAXIMUM CELL DIMENSI,
* 4HON =, F10.5, 8H RADIANS)
C
C CALCULATE THE ANGULAR LIMITS FOR RADIAL ZONES
C
C ETA1 = ATAN(R1/AP(3))
C ETA2 = ATAN(R2/AP(3))
```



```

AAA = ETA2 - ETA1
C
C CALCULATE NUMBER AND ANGULAR WIDTH OF RADIAL ZONES
C
NETA = INT(AAA/DANG) + 1
IF (NETA.LE.MRADZ) GO TO 10
WRITE (NOUT,99998) NETA
99998 FORMAT (4X, 37HMAX NO. RADIAL ZONES EXCEEDED. NETA =, I5)
STOP 4
10 CONTINUE
DETA = AAA/NETA
C
C FIND PHI INTERVALS AND NUMBER OF INTERVALS.
C
BBB = PHI2 - PHI1
DO 20 I=1,NETA
ETA = ETA1 + DETA*FLOAT(I)
ZWI = (COS(DANG)-COS(ETA)**2)/SIN(ETA)**2
DD = ACOS(ZWI)
C
C NUMBER (NPHI) AND AZIMUTHAL WIDTH (DELY) OF CELLS IN
C RADIAL ZONE I
C
NPHI(I) = INT(BBB/DD) + 1
DELY(I) = BBB/NPHI(I)
20 CONTINUE
C
C CALCULATE NTOT (I), THE CUMULATIVE INDEX USED BY CELNUM
C UP TO START OF RADIAL CELL NUMBER I
C
NTOT(1) = 0
DO 30 I=2,NETA
NTOT(I) = NTOT(I-1) + NPHI(I-1)
30 CONTINUE
C
C TOTAL NUMBER OF CELLS - NCEL
C
NCEL = NTOT(NETA) + NPHI(NETA)
IF (NCEL.LE.MNTOT) GO TO 40
WRITE (NOUT,99997) NCEL
99997 FORMAT (5X, 40HMAXIMUM NUMBER OF CELLS EXCEEDED. NCEL =, I5)
STOP 6
40 CONTINUE
WRITE (NOUT,99996) NETA, DETA
99996 FORMAT (10X, 28HNUMBER OF RADIAL INTERVALS =, I4, /, 10X,
* 18HANGULAR INTERVAL =, F10.5, 8H RADIANS, /, 4X, 11HRADIAL ZONE,
* 2X, 17HNO. CELLS IN ZONE, 2X, 17HANG WIDTH AZ ZONE)
DO 50 I=1,NETA
WRITE (NOUT,99995) I, NPHI(I), DELY(I)
50 CONTINUE
99995 FORMAT (10X, I5, 5X, I10, 5X, F10.4)
WRITE (NOUT,99994) NCEL
99994 FORMAT (10X, 25HTOTAL NUMBER OF CELLS IS , I4)
C
C CYCLE OVER HELIOSTATS, ASSIGNING CELL NUMBERS
C
REWIND 1
READ (1) NHEST
NHEST IS THE NUMBER OF HELIOSTATS
C
REWIND 2
DO 80 NH=1,NHEST
READ (1) X, Y, Z
ID = NH
AZT = Y - AP(2)
AUT = X - AP(1)
IF (AZT.EQ.0. .AND. AUT.EQ.0.) GO TO 60
PHI = ATAN2(AZT,AUT)
SQR = AZT**2 + AUT**2
GO TO 70
60 PHI = 0.
SQR = 0.
70 ETA = ATAN(SQR/(AP(3)-Z))
SQR = SQR + (AP(3)-Z)**2
CALL CELNUM(ETA, PHI, ETA1, PHI1, DETA, NETA, JJ)
WRITE (2) ID, X, Y, Z
80 CONTINUE
REWIND 2
C
C ARRANGE HELIOSTATS ON TAPE 4 BY CELL NUMBER, FIND CENTROID
C
REWIND 3
REWIND 4
DO 130 I=1,NCEL
Q1 = 0.
Q2 = 0.
Q3 = 0.
NOHIC = 0
REWIND 2
REWIND 3

```

```

DO 90 NH=1,NHST
  READ (2) ID, X, Y, Z, JJ
  IF (JJ.NE.1) GO TO 90
  WRITE (3) ID, X, Y, Z, JJ
  NOHIC = NOHIC + 1
  Q1 = Q1 + X
  Q2 = Q2 + Y
  Q3 = Q3 + Z
90  CONTINUE
  IF (NOHIC.EQ.0) GO TO 100
  Q1 = Q1/FLOAT(NOHIC)
  Q2 = Q2/FLOAT(NOHIC)
  Q3 = Q3/FLOAT(NOHIC)
100  IF (NOHIC.LE.MNHIC) GO TO 110
  WRITE (NOUT,99993) NOHIC,I
99993  FORMAT (5X, 35HMAX NO. HELIOSTATS IN CELL EXCEEDED, 2X,
  * 8HNOHIC = , 16, 2X, 9HCELL NO.=, I4)
  STOP 6
110  WRITE (4) I, NOHIC, Q1, Q2, Q3
  IF (IPRINT.EQ.1) WRITE (NOUT, 111) I, NOHIC, Q1, Q2, Q3
111  FORMAT(2X,2I5,3F15.2)
  IF (NOHIC.EQ.0) GO TO 130
  REWIND 3
  DO 120 NH=1,NOHIC
  READ (3) ID, X, Y, Z, JJ
  WRITE (4) ID, X, Y, Z, JJ
120  CONTINUE
130  CONTINUE
  REWIND 1
  REWIND 2
  REWIND 3
  REWIND 4
C
C  ORDER HELIOSTATS IN INCREASING DISTANCE FROM CENTROID
C  IN EACH CELL
C
C  INSERT PLOT INFORMATION AT BEGINNING OF TAPE 3
C
  WRITE (3) NETA
  WRITE (3) ETA1, DETA, (AP(I),I=1,3), (NPHI(I),I=1,NETA),
  * (DELY(I),I=1,NETA), PHI1, PHI2, R2
C
  WRITE (3) NCEL
  DO 170 I=1,NCEL
  READ (4) NC, NOHIC, Q1, Q2, Q3
  WRITE (3) NC, NOHIC, Q1, Q2, Q3
  IF (NOHIC.EQ.0) GO TO 170
C
C  TRANSFER INFORMATION FOR ONE CELL ONTO TAPE 2
C
  REWIND 2
  DO 140 N=1,NOHIC
  READ (4) ID, X, Y, Z, JJ
  IF (JJ.NE.1) STOP 22
  ZIC(N) = (X-Q1)**2 + (Y-Q2)**2 + (Z-Q3)**2
  IDH(N) = ID
  WRITE (2) ID, X, Y, Z, JJ
140  CONTINUE
C
C  SORT IN ORDER OF INCREASING ZIC
C
  CALL SSORT(ZIC, IDH, NOHIC, 2)
C
C  PUT HELIOSTATS IN NEW ORDER ON TAPE 3
C
  DO 160 N=1,NOHIC
  REWIND 2
  IDA = IDH(N)
150  READ (2) ID, X, Y, Z, JJ
  IF (ID.NE.IDA) GO TO 150
  WRITE (3) ID, X, Y, Z, JJ
160  CONTINUE
170  CONTINUE
  IF (IPRINT.NE.1) GO TO 200
  REWIND 3
  READ (3) NETA
  READ (3) ETA1, DETA, (AP(I),I=1,3), (NPHI(I),I=1,NETA),
  * (DELY(I),I=1,NETA), PHI1, PHI2, R2
  READ (3) NCEL
  DO 190 I=1,NCEL
  READ (3) NC, NOHIC, Q1, Q2, Q3
  WRITE (NOUT,99992) NC, NOHIC, Q1, Q2, Q3
99992  FORMAT (/, 5X, 11HCELL NUMBER, 15, 5X, 20HNUMBER OF HELIOSTATS,
  * 15, /, 5X, 25HCOORDINATES OF CENTROID =, 3F10.3)
  IF (NOHIC.EQ.0) GO TO 190
  DO 180 N=1,NOHIC
  READ (3) ID, X, Y, Z, JJ
  WRITE (NOUT,99991) ID, X, Y, Z
180  CONTINUE
99991  FORMAT (5X, 3HID=, 15, 2X, 6HX,Y,Z=, 3F10.3)

```

190 CONTINUE  
200 CONTINUE

C  
END

C  
C  
SUBROUTINE CELNUM(X, Y, X1, Y1, DX, NX, JJ)  
C FINDS CELL NUMBER JJ CORRESPONDING TO ANGULAR POSITION (X,Y)  
C OF A HELIOSTAT WHERE X IS THE ANGLE IN RADIANS FROM THE DOWNWARD  
C AXIS OF THE TOWER TO A LINE CONNECTING THE AIM POINT TO THE  
C HELIOSTAT. Y IS THE AZIMUTHAL COORDINATE IN RADIANS OF THE  
C HELIOSTAT. X1 IS A LOWER BOUND ON X AND Y1 A LOWER BOUND ON  
C Y FOR THE FIELD OF HELIOSTATS. DX IS THE INTERVAL IN THE X ANGLE  
C AND NX THE CORRESPONDING NUMBER OF INTERVALS. THE NUMBER OF  
C Y INTERVALS VARIES WITH X AND IS SUPPLIED IN COMMON/CCEL/.  
COMMON /CCEL/ ETA1, ETA2, DELTA, NPHI(15), DELY(15)  
COMMON /WK/ NTOT(120)  
JX = INT(ABS(X-X1)/DX) + 1  
JX = MIN0(JX,NX)  
JY = INT(ABS(Y-Y1)/DELY(JX)) + 1  
JJ = NTOT(JX) + MIN0(JY,NPHI(JX))  
RETURN  
END

**DISTRIBUTION:**

The Aerospace Corporation  
Solar Thermal Projects  
Energy Systems Group  
P. O. Box 92957  
Los Angeles, CA 90009  
Attn: L. Katz, Director

Department of Energy  
Solar Thermal Power Systems  
Central Solar Energy Division  
Washington, DC 20545  
Attn: G. W. Braun, Assistant Director

Department of Energy  
Large Solar Thermal Power Systems  
Central Solar Energy Division  
Washington, DC 20545  
Attn: G. M. Kaplan, Acting Chief

Department of Energy  
Solar Geothermal and Electric Energy  
Energy Technology Division  
Washington, DC 20545  
Attn: H. H. Marvin, Deputy Program Director

GESER  
Ecole Centrale des Arts et Manufactures  
Grande Voie des Vignes  
92290 Chatenay - Malabry  
France  
Attn: C. Ouannes

Department of Energy  
Large Power Systems Branch  
Central Power Systems Division  
Washington, DC 20545  
Attn: J. P. Zingesser

Department of Energy (3)  
Solar Energy Division  
San Francisco Operations Office  
1333 Broadway, Wells Fargo Building  
Oakland, CA 94612  
Attn: J. A. Blasy, Director  
R. W. Hughey, Deputy Div. Director  
S. D. Elliott

Department of Energy STMPO  
Suite 210  
9650 Flair Park Drive  
El Monte, CA 91731  
Attn: R. N. Schweinberg

Electric Power Research Institute  
3412 Hillview Avenue  
P. O. Box 10412  
Palo Alto, CA 94304  
Attn: J. Bigger

NASA-Lewis Research Center  
21000 Brookpark Road  
Cleveland, OH 44135  
Attn: B. Masica

Public Service of New Mexico  
P. O. Box 2267  
Albuquerque, NM 87103  
Attn: J. Maddox

Indian Institute of Technology  
Solar Energy Group  
Centre of Energy Studies  
Hauz Khas, New Delhi-110029, India  
Attn: A. K. Seth

McDonnell Douglas Astronautics Co. (3)  
5301 Bolsa  
Huntington Beach, CA 92647  
Attn: R. H. McFee  
J. B. Blackman  
J. R. Campbell

Swiss Federal Institute for Reactor Research  
5303 Wurenlingen  
Switzerland  
Attn: P. Kesselring

Sanders Associates (2)  
MER 12 1214  
95 Canal Street  
Nashua, NH 03060  
Attn: S. B. Davis  
N. McHugh

Belgonucleaire  
Societe Anonyme  
Rue de Champ de Mars 25  
B -1050 Bruxelles  
Belgium  
Attn: J. P. Fabry, Ingenieur

DFVLR  
Pfaffenwaldring 38  
7000 Stuttgart 80  
Federal Republic of Germany  
Attn: K. J. Erhardt

**DISTRIBUTION (cont):**

INITEC  
Padilla 17  
Madrid-6  
Spain  
Attn: F. Delgado

Head of Energy and Thermal Control Dept. (2)  
Construcciones Aeronauticas, S. A.  
CASA Space Division  
Rey Francisco, 4  
Madrid-8 Apartado 193  
Spain  
Attn: A. Escarda

Snamprogetti  
20097 S. Donato Milanese  
Milano, Italy  
Attn: A. D. Benedetti

Indian Institute of Technology  
Dept. of Physics  
New Delhi-29, India  
Attn: R. N. Singh

C. T. I. P. International  
30 Rockefeller Plaza  
New York, NY 10020  
Attn: C. Mazzolini

Israel Institute of Technology  
Faculty of Mechanical Engineering  
Technion City, Haifa 32000  
Israel  
Attn: G. Grossman

Foster Wheeler Development Corp.  
12 Peach Tree Hill Road  
Livingston, NJ 07039  
Attn: G. D. Gupta

Solar Energy Research Institute (4)  
Resource Assessment Branch  
1536 Cole Boulevard  
Golden, CO 80401  
Attn: R. Hulstrom  
J. Williamson  
B. Butler  
K. Touryan

General Electric (2)  
1 River Road, Building 23, Room 334  
Schenectady, NY 12345  
Attn: R. H. Horton  
W. F. Knightly

General Electric (2)  
1 River Road, Building 6, Room 329  
Schenectady, NY 12345  
Attn: S. Schwartz  
T. Curinga

Georgia Institute of Technology (2)  
Solar Energy & Materials Technology Div.  
Engineering Experiment Station  
Atlanta, GA 30322  
Attn: C. T. Brown  
P. Mackie

Black & Veatch (3)  
P. O. Box 8405  
Kansas City, MO 64114  
Attn: M. Wolf  
S. L. Levy  
J. T. Davis

University of Houston  
Solar Energy Laboratory  
4800 Calhoun  
Houston, TX 77004  
Attn: Fred Lipps  
L. Vant-Hull

Acurex Corporation (3)  
Alternate Energy Division  
Aerotherm Group  
485 Clyde Avenue  
Mountain View, CA 94042  
Attn: P. Overly  
D. Brink  
D. R. McCullough

S. C. Plotkin & Associates  
6451 W. 83rd Street  
Los Angeles, CA 90045  
Attn: W. H. Raser

Westinghouse Advanced Energy (6)  
Systems Division  
P. O. Box 10864  
Pittsburgh, PA 15236  
Attn: J. Day  
D. Hofer  
M. Lipner  
W. Parker  
W. Pierce  
C. Silverstein

**DISTRIBUTION (cont):**

General Electric Company  
Space Division  
Room 7246 CC&F #7  
P. O. Box 8555  
Philadelphia, PA 19101  
Attn: A. J. Poche

Jet Propulsion Laboratory (4)  
4800 Oak Grove Drive  
Pasadena, CA 91103  
Attn: P. Poon, MS 506-328  
K. C. Bordoloi, MS 506-328  
V. Truscillo, MS 502-201  
I. Khan, MS 506-328

Martin Marietta (6)  
P. O. Box 179  
Denver, CO 80201  
Attn: W. Hart, MS S0510  
G. A. Roe, MS S0510  
P. Norris, MS C0403  
J. Montague, MS C0403  
T. Oliver, MS S0403  
B. Zuver, MS S8120

Dynatherm Corporation  
One Industry Lane  
Cockeysville, MD 21030  
Attn: D. Wolfe

Gruman Energy Systems  
4175 Veterans Memorial Highway  
Ronkonkoma, NY 11779  
Attn: G. Yenatchi

Bechtel Corporation  
P. O. Box 3965  
San Francisco, CA 94119  
Attn: R. L. Lessley, 301-3

University of Minnesota  
Department of Electrical Engineering  
139 Electrical Engineering  
123 Church Street, SE  
Minneapolis, MN 55455  
Attn: M. Riaz

University of Louisville  
Department of Electrical Engineering  
Louisville, KY 40208  
Attn: K. C. Bordoloi

F. A. Blake  
7102 South Franklin Street  
Littleton, CO 80122

Boeing Engineering and Construction (2)  
P. O. Box 3707  
Seattle, WA 98124  
Attn: B. Beverly, MS 9A-47  
E. J. Valley

Boeing Engineering and Construction  
625 W. Andover Park  
Tukwila, WA 98188  
Attn: F. Mahony

Booz, Allen & Hamilton, Inc.  
8801 E. Pleasant Valley Road  
Cleveland, OH 44131  
Attn: C. G. Howard

New Mexico State University  
Dept. of Mechanical Engineering  
P. O. Box 3450  
Las Cruces, NM 81803  
Attn: G.P. Mulholland

Airesearch Manufacturing Co. of California  
Dept 38 Mail Stop T-40  
2525 W. 190th Street  
Torrance, CA 90509  
Attn: T. S. Smith

University of Waterloo  
Electrical Engineering Department  
Waterloo, Ontario  
Canada  
Attn: L. Y. Wei

Ohio State University  
Department of Mechanical Engineering  
206 W. 18th Avenue  
Columbus, OH 43210  
Attn: T. Pettenski

Veda Inc.  
Building D  
400 North Mobil  
Camarillo, CA 93010  
Attn: R. V. Vener

Purdue University  
Dept. of Mechanical Engineering  
Lafayette, IN 47907  
Attn: L. K. Matthews

University of Illinois  
Department of General Engineering  
117 Transportation Building  
Urbana, IL 61801  
Attn: O. Coskunoglu

DISTRIBUTION (cont):

1521 J. L. Mortley  
1537 N. R. Keltner  
1550 F. W. Neilson  
1556 E. A. Igel  
4200 G. Yonas  
4210 J. B. Gerardo  
4230 J. E. Powell  
4231 T. P. Wright  
4231 F. Biggs  
4231 R. E. Lighthill  
4231 C. N. Vittitoe (25)  
4240 G. W. Kuswa  
4250 T. H. Martin  
4700 J. H. Scott  
4710 G. E. Brandvold  
4713 J. V. Otts  
4713 D. L. King  
4713 W. K. Bell  
4713 D. B. Davis  
4713 J. T. Holmes  
4713 L. O. Seamons  
4713 M. C. Stoddard  
4716 J. F. Banas  
4716 R. W. Harrigan  
4716 G. W. Treadwell  
4717 J. A. Leonard  
4717 E. L. Harley  
4721 J. C. Zimmerman  
4723 T. A. Dellin

4723 R. R. Peters  
4724 B. D. Shafer  
5513 R. J. Gross  
5523 J. R. Koterak  
8124 M. J. Fish  
8324 J. D. Hankins  
8331 P. L. Leary  
8334 R. Y. Lee  
8430 R. C. Wayne  
8431 P. J. Eicker  
8450 C. S. Selvage  
8451 C. S. Selvage(Actg.)  
8451 T. D. Brumleve  
8451 C. J. Pignolet  
8452 A. C. Skinrood  
8452 D. L. Atwood  
8452 A. F. Baker  
8452 L. V. Griffith  
8452 C. L. Yang  
8453 W. G. Wilson  
8453 E. T. Cull  
8453 P. De Laquil  
8214 M. A. Pound  
3141 L. J. Erickson (5)  
3151 W. L. Garner (3)

For: DOE/TIC (Unlimited Release)

DOE/TIC (25)

(C. H. Dalin 3154-3)